journal of the international meteor organization

WGN

36:4
august 2008

Perseids
Image intensifiers
Meteoroid flux
Video meteors

ISSN 1016-3115

WGN Vol. 36, No. 4, August 2008, pp. 67 – 92

Administrative

Perseids

Ongoing meteor work

Preliminary results

Front cover photo

A sporadic fireball photographed in 2008 by Krysztof Polakowski in Gniewowo.

Writing for WGN This Journal welcomes papers submitted for publication. All papers are reviewed for scientific content, and edited for English and style. Instructions for authors can be found in WGN **31:4**, 124–128, and at `http://www.imo.net/articles/writingforwgn.pdf` .

Legal address International Meteor Organization, Mattheessensstraat 60, 2540 Hove, Belgium.

Editorial — Changes to WGN

Chris Trayner

When I started the Editorship of WGN I agreed to do it for five years; I have now done it for nearly six. It was announced in an earlier WGN that I intend to step down. A job description for Editor was put out earlier and applications were solicited. We had relatively few enquiries, and none from candidates with the experience we need. Thus no appointment could be made from the applications received. Nonetheless, the IMO Council is grateful to all those who expressed interest and to those who sent us their thoughts.

Many hands make light work

Our ideas have evolved: Council is now of the opinion that the job is too large for one individual. (That this is true of me can be seen in the lamentable lateness of the recent issues.) Our thinking now is that WGN should be edited by a team comprising an Editor in Chief, a Production Editor and several Handling Editors.

This is easy to say but harder to make work: there are many things to get right, both large and small. One requirement is that the team is large enough that the workload for each member is small enough. We already have probably enough volunteers for that, so people joining the team will only have a reasonable number of papers to edit each year. It may also mean that the Handling Editors can concentrate on papers which interest them.

These Handling Editors will handle individual articles, but someone has to take overall charge of the Journal. This will include deciding what is published, communicating with Handling Editors and generally co-ordinating the work. This post is called Editor-in-chief and someone has indicated their willingness to do this job.

What abilities must an Handling Editor have?

Less than you might think! When I started I had no experience of editing. I knew far less about meteors than the people who help me. The main requirement is enthusiasm (and of course some meteor knowledge).

Nor is excellent English needed — we have several native English speakers who can advise, and may act as an email help desk for English. If you want to improve your English this could be a pleasant way to do it, reading and sometimes writing about astronomy.

There will be style files or equivalent to help arrange articles in the correct format.

If you think you might be interested in joining in the editing, please contact us, telling us how many articles per year you feel able to edit. Email `wgn@imo.net`, putting the word Meteor in the subject line to get past the anti-spam filters.

Word processor format

WGN is produced in LaTeX, and up till now anyone helping with the editing has had to understand this. This will change: Andre Knöfel edits Meteoros, the AKM Journal, in a mixture of LaTeX and Microsoft Word. Any one article is edited in one of these two and exported as PDF. The entire Journal is put together by combining articles at the PDF level. Andre Knöfel has much experience of this, and WGN will be produced like this.

This will mean that editors can work in Word if they prefer. It should also speed up the editing of articles submitted in Word, which currently have to be reformatted into LaTeX.

Andre Knöfel has agreed to take on the job of Production Editor: he will combine the various parts into the whole. The IMO Council is very grateful to him for this. This way of working may not start immediately.

A rough timetable

The intention is that the new team mechanism will be used starting with the next issue, i.e. October (36:5). The full mechanism (which will include a web-based management tool) will not be in place until the start of 2009 at the earliest. This will also give time for the team to find comfortable ways of working.

There will be many editors new to the job, and no doubt mistakes will be made. Our hope is that they will be minor: fonts slightly different, columns of slightly different widths, and so on. This will improve as people learn. At IMC Marc Gyssens learned that the English expression for this is 'to get the wrinkles out', and I learned that the Belgian expression is 'to get the children's' diseases out'. The mistakes are unlikely to be as bad as the one I made in my first issue (31:1) where the section numbers ran straight through the entire issue, rather than starting at 1 for each article. We hope you will be patient as the new team 'learns the ropes', to use another English expression.

IMO bibcode WGN-364-editorial NASA-ADS bibcode 2008JIMO...36...67T

Perseids

Filament and dust trail encounters and the mean Perseid maximum 2000–2007

Jürgen Rendtel [1]

The Perseid returns in the period 2000–2007 are analysed using global visual data collected by the IMO. We present profiles of the population index r and the ZHR for the near-maximum period 138°5–141°5 for each return. The average maximum occurs at $\lambda_\odot = 140°11 \pm 0°1$ with a ZHR of 81 ± 8. An additional peak was observed in 2002 at $139°82 \pm 0°02$. The strong but short-lived peak at $\lambda_\odot = 139°450 \pm 0°010$ in 2004 is associated with the encounter of the 4-revolution dust trail of 109P/Swift-Tuttle. This trail can also be detected in 2005 and may be in the 2007 data about 0°15 before the predicted location. The 2007 Perseid data also show the encounter with meteoroids in orbits resonant with Jupiter.

Received 2008 June 20

1 Introduction

The Perseids continue to attract the attention of meteor observers, especially after the end of the series of intense Leonid returns. Annual analyses of the global visual data until 1999 have been published (Rendtel and Arlt, 1999) and later only for the Perseid returns of 2000 (Arlt and Händel, 2000) and 2002 (Arlt and Buchmann, 2002). Observations of the peculiar peak in 2004 using different observing methods have been reported (e.g. Arlt, 2004; Berinde et al., 2004; Dubietis, 2004; Kac, 2004; Miskotte and Johannink, 2004; Trigo-Rodriguez et al., 2005) but no analysis of the global data was published in WGN.

The Perseid meteoroid stream is composed of different components (Jenniskens, 2006): (i) meteoroids from different ejection periods which have seen many perturbations over time and hence can cross the Earth's orbit at different positions — a so-called background component; (ii) meteoroids in dust trails formed not too many orbital periods ago and — although perturbed as well — still in a reasonably small band at least when approaching their perihelia close to the Earth's orbit; (iii) older dust accumulated and kept in mean-motion resonances with Jupiter, called a filament (Jenniskens et al., 1998).

2 Observing conditions and data analysis

The so-called traditional maximum occurs with rather little variation in position and strength. Its position is close to $\lambda_\odot = 140°1$. The observing conditions for this time are listed in Table 1. Considering that the radiant reaches its highest position in the sky after local midnight, the data of the 2000, 2001, 2003 and 2006 returns are expected to be strongly affected by moonlight.

Despite the very different conditions, we applied the standard analysis procedure to all data sets. Of course, we have to adapt the interval lengths and sample sizes for each subset to the annual data sample. This is described in the respective section for each return.

Table 1 – Time of the mean Perseid maximum and the influence of moonlight on visual observations in the period 2000–2007.

Year	Time (UT) of $\lambda_\odot = 140°1$	Preferred region	Lunar phase
2000	Aug 12, 13^h	Pacific	93% +
2001	Aug 12, 19^h	Asia	41% −
2002	Aug 13, 01^h	Europe	29% +
2003	Aug 13, 07^h	America	98% −
2004	Aug 12, 13^h	Pacific	9% −
2005	Aug 12, 20^h	Asia	52% +
2006	Aug 13, 02^h	Europe	78% −
2007	Aug 13, 08^h	America	2% +

The reports on the global analyses of visual data usually come with a detailed table of the contribution of the observers. Since we analysed data of eight consecutive returns here, these tables would have filled many pages. Therefore, we restrict to summaries of the samples per return (Table 2). The total sample of 195 086 Perseids was collected by 1135 observers over 11 928 hours effective observing time, comprising data in 23 597 count intervals. The respective numbers are 159 560 Perseid meteors reported within 17 010 intervals by 979 observers over 5667 hours in the near-maximum period. Details can be taken from the files of the Visual Meteor DataBase (VMDB) of the IMO which is available on the IMO's web page (`www.imo.net`). Further, we restrict our analysis here to the near maximum period between $\lambda_\odot = 138°5$ and $141°5$. This includes the mean maximum as well as periods where additional activity was expected.

The analysis of the population index r is the first step of a shower activity analysis as it allows us to correct for the number of meteors visible under standard observing conditions. This is done for the data sets of each return, again concentrated in the near-maximum period between $\lambda_\odot = 138°5$ and $141°5$ only. The values of the population index r outside this interval can be assumed to vary little from one year to the next. For

[1]Eschenweg 16, 14476 Marquardt, Germany.
Email: `jrendtel@aip.de`

IMO bibcode WGN-364-rendtel-perseids
NASA-ADS bibcode 2008JIMO...36...68R

Table 2 – Summary of the Perseid data per year in the period 2000–2007. Total refers to the entire activity period; columns 3–6 and 3–8 give the net observing time (T_{eff}), the number of Perseids (PER) and the number of count intervals in the entire activity period and the near-maximum period ($138\overset{\circ}{.}5$–$141\overset{\circ}{.}5$).

Year	Observers	Entire activity period			Near maximum period		
	(Total)	T_{eff}	PER	Int.	T_{eff}	PER	Int.
2000	441	3685	30692	3713	882	17675	1071
2001	328	2755	25263	3072	804	17033	1122
2002	298	1645	30484	2763	843	24484	1882
2003	145	1256	7825	1376	292	3592	397
2004	361	2072	61629	8124	1376	57241	7402
2005	327	2083	39623	5263	1020	29369	3842
2006	131	1009	5248	1258	196	2536	417
2007	78	472	8915	1164	253	7630	886
All	1135	11928	195086	23597	5667	159560	17010

Table 3 – Bin length and sample size used for the calculation of the population index profiles from visual observations in the years 2000–2007. The data points in the Figures represent data of count intervals put together until either the minimum number of shower meteors or the maximum bin length is reached. The minimum shower meteor number is set to 100 Perseids. (In 2002 the data coverage in the immediate peak period was very good and, because we are interested in structures in just that period, the limit for 2002 was increased to 200 to produce lower error margins.) The numbers in the last column may be smaller than in Table 2 when magnitude data were combined for several count intervals.

Year	Interval	Bin length	#Bins
2000	$138\overset{\circ}{.}5$–$141\overset{\circ}{.}5$	$0\overset{\circ}{.}2$	917
2001	$138\overset{\circ}{.}5$–$141\overset{\circ}{.}5$	$0\overset{\circ}{.}2$	988
2002	$138\overset{\circ}{.}5$–$141\overset{\circ}{.}5$	$0\overset{\circ}{.}2$	1131
2003	$138\overset{\circ}{.}5$–$141\overset{\circ}{.}5$	$0\overset{\circ}{.}2$	346
2004	$138\overset{\circ}{.}5$–$139\overset{\circ}{.}3$	$0\overset{\circ}{.}2$	4497
	$139\overset{\circ}{.}3$–$139\overset{\circ}{.}7$	$0\overset{\circ}{.}05$	
	$139\overset{\circ}{.}7$–$141\overset{\circ}{.}5$	$0\overset{\circ}{.}2$	
2005	$138\overset{\circ}{.}5$–$139\overset{\circ}{.}2$	$0\overset{\circ}{.}2$	2797
	$139\overset{\circ}{.}2$–$139\overset{\circ}{.}4$	$0\overset{\circ}{.}1$	
	$139\overset{\circ}{.}4$–$140\overset{\circ}{.}1$	$0\overset{\circ}{.}2$	
	$140\overset{\circ}{.}1$–$140\overset{\circ}{.}3$	$0\overset{\circ}{.}08$	
	$140\overset{\circ}{.}3$–$141\overset{\circ}{.}5$	$0\overset{\circ}{.}2$	
2006	$138\overset{\circ}{.}5$–$141\overset{\circ}{.}5$	$0\overset{\circ}{.}2$	417
2007	$138\overset{\circ}{.}5$–$141\overset{\circ}{.}5$	$0\overset{\circ}{.}2$	558

detailed investigation of other periods, the respective values of r need to be determined.

Table 3 lists the data and parameters for the r-profiles of the individual returns. Generally, we excluded data obtained under very poor circumstances from the analysis. For the magnitude data which is used for the calculation of r we omitted those obtained when the limiting magnitude was below $m = +5.5$.

We show the r-profiles together with the rate profiles later to allow association between features in the two profiles connected with possible mass sorting effects in the stream, especially in the filaments and outburst portions. If we look for structures in the profiles and try to identify local minima or maxima with the encounter of specific stream sections, we have to bear in mind that the major portion of the meteors comes from the annual mean maximum component. If the Earth encounters a trail with a different particle size distribution, the observable change in r is small and is a superposition of the mean and trail meteoroids.

For the calculation of the ZHR and the respective profiles, we follow the procedure as described by Arlt (2004).

3 Peculiarities of the annual returns

The mean maximum occurs near $\lambda_{\odot} = 140\overset{\circ}{.}1$. Additional peaks have been observed in the period between 1988 and 1999 (Brown and Rendtel, 1996; Jenniskens et al., 1998; Arlt, 1998; Rendtel and Arlt, 1999). Then the series of dense stream portion encounters ended, and there was no sign of an additional peak in 2000 (Arlt and Händel, 2000).

A third peak after the filament and mean maxima was found in the data of the Perseid returns of 1997–1999 (Arlt, 1998; Arlt, 1999; Rendtel and Arlt, 1999) at $\lambda_{\odot} = 140\overset{\circ}{.}35$ (1997 and 1998) or $\lambda_{\odot} = 140\overset{\circ}{.}45$ (in 1999) with a ZHR between 68 and 80.

3.1 Moonlit return 2000

Despite the full moon shortly after the maximum, the selected interval between $\lambda_{\odot} = 138\overset{\circ}{.}5$ and $141\overset{\circ}{.}5$ is well covered with observational data, although the average limiting magnitudes are mainly below $m = +6.0$, reducing the size of the data samples. Consequently, both the profiles of r and ZHR are limited regarding their temporal resolution. Thus it is not possible to search for fine structures. The population index profile (Figure 1) shows a distinct minimum of $r = 1.84 \pm 0.02$ essentially at the location of the mean rate maximum near $140\overset{\circ}{.}0$ and a pronounced peak of $r = 2.28 \pm 0.16$ shortly thereafter, followed by a steady decrease to about 2.0 at the end of the maximum period.

In the same interval, the ZHR rises more or less continuously to the peak ZHR $= 97.2 \pm 3.4$ at $\lambda_{\odot} = 139\overset{\circ}{.}979$ (Figure 2). Considering the amount of data,

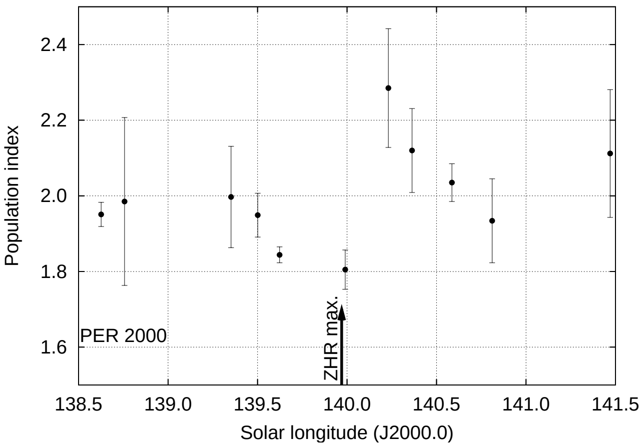

Figure 1 – Population index profile of the Perseids 2000. The arrow indicates the position of the ZHR maximum.

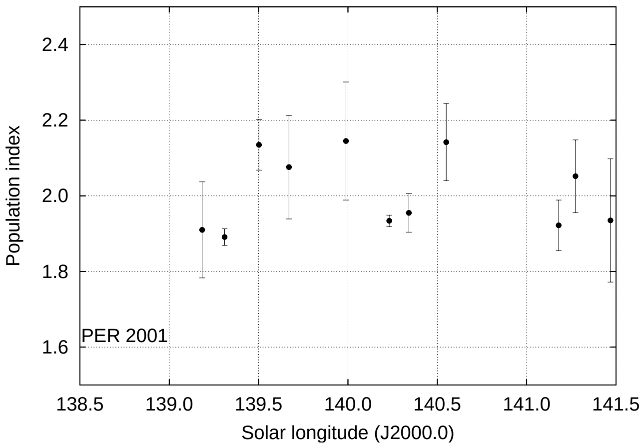

Figure 3 – Population index profile of the Perseids 2001. No significant structure or minimum occurs.

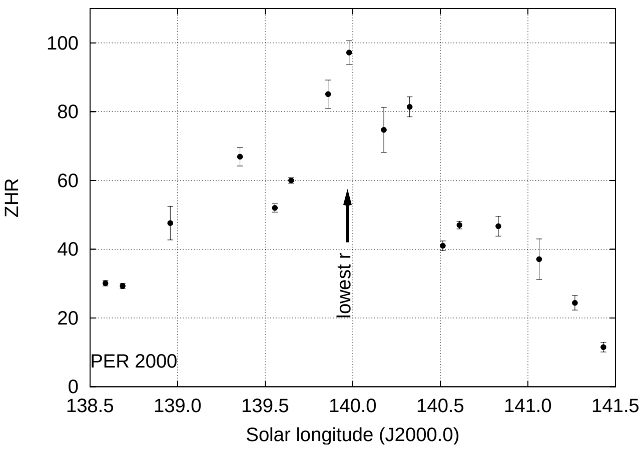

Figure 2 – Profile of the ZHR for the Perseids 2000 based on the r-profile shown in Figure 1. The arrow marks the position where the lowest r was calculated.

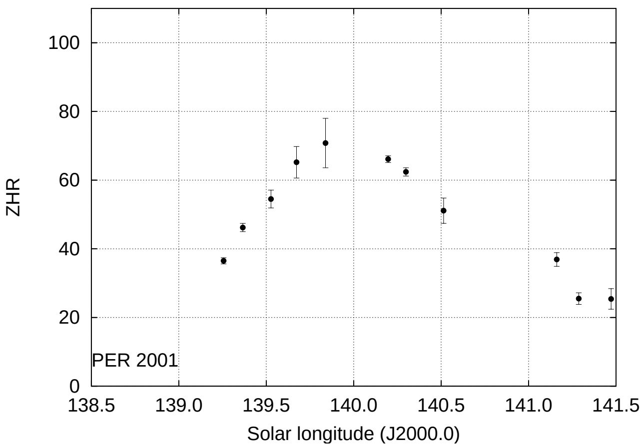

Figure 4 – The ZHR profile of the 2001 Perseid return shows a broad mean maximum. The r-profile shown in Figure 3 was used.

we cannot give detailed information whether the maximum at $\lambda_\odot = 139\overset{\circ}{.}36$ (ZHR = 67 ± 3) can be associated with the filament peaks observed in the preceeding years. At least there is some doubt because the average sporadic rate of the same bin is by a factor of about 1.5 higher than the rates in the neighbouring intervals.

The third peak described above might be in the present in the profile at $\lambda_\odot$=$140\overset{\circ}{.}33$. Again, the amount of data does not allow to go into shorter details and therefore we cannot exclude the possibility that we just find a broad mean maximum with a ZHR > 60 between $139\overset{\circ}{.}65$ and $140\overset{\circ}{.}4$.

3.2 Smooth profile in 2001

Observing conditions for a maximum shortly after the last quarter moon are partly affected. The population index profile (Figure 3) shows no distinct structure. The only significant feature is a minimum of $r = 1.93 \pm 0.02$ around $\lambda_\odot = 140\overset{\circ}{.}2$, probably associated with the mean maximum period. This moment corresponds with the start of most European observing activities after a gap in our data in the roughly six hours before. The ZHR profile (Figure 4) is quite smooth with no signs of additional peaks. The result shows that the filament peak has definitively disappeared, as did the third peak.

3.3 Additional peak in 2002

For this Perseid return, which occurred under favourable conditions regarding the moonlight disturbance, a detailed analysis has been published by Arlt and Buchmann (2002). We included the data set in this work for completeness and to apply consistent procedures for all returns between 2000 and 2007. The population index (Figure 5) is relatively low over the entire period shown here. r is comparable with the figure of the 2000 maximum. Although the r-profile is smooth and the observations were done under good conditions in terms of the limiting magnitude, we find a distinct rate peak of ZHR = 110 ± 7 at $\lambda_\odot = 139\overset{\circ}{.}8$ (Figure 6). For the analysis we limited the bin length to $0\overset{\circ}{.}08$ shifted by $0\overset{\circ}{.}04$ (approximately 1 hour resolution). This peak is not visible in the analysis of Arlt and Buchmann (2002). The two intervals with these high rates show neither a deviation of the sporadic rate from the other intervals nor a poorer limiting magnitude. Furthermore, the Perseid radiant is at least 30° above the horizon at the locations of the contributing observers. The mean maximum occurs at $\lambda_\odot = 140\overset{\circ}{.}13$ with a ZHR of 74 ± 3. Assuming a smooth ZHR profile of the mean maximum rate, we find a contribution of about 40 coming from the peak. That makes about half the strength of the usual ZHR. Since we cannot locate

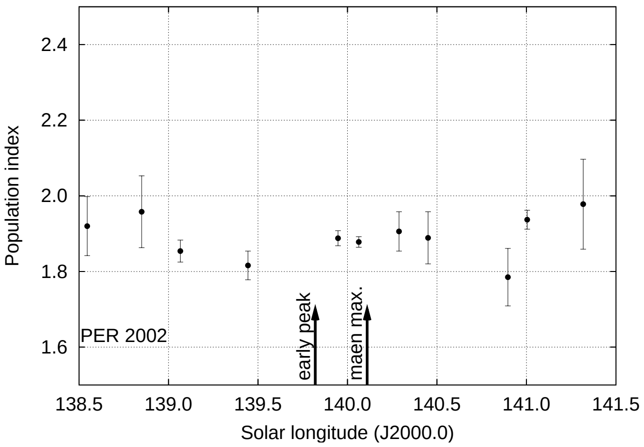

Figure 5 – Population index profile of the Perseids 2002. Arrows mark the positions of the observed early ZHR peak and the mean maximum.

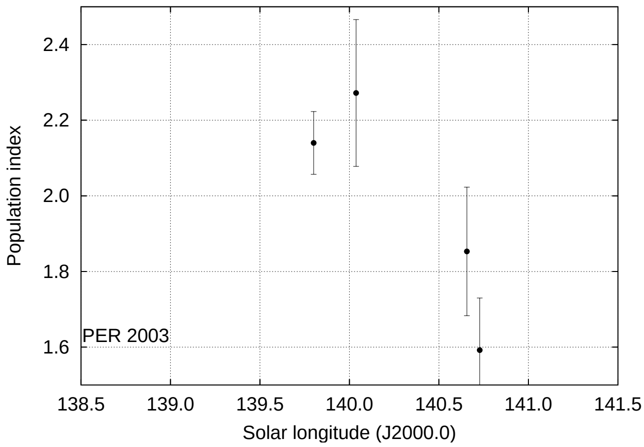

Figure 7 – In 2003 the poor circumstances did not allow the determination of a reliable r-profile. The values are higher than those obtained under better conditions.

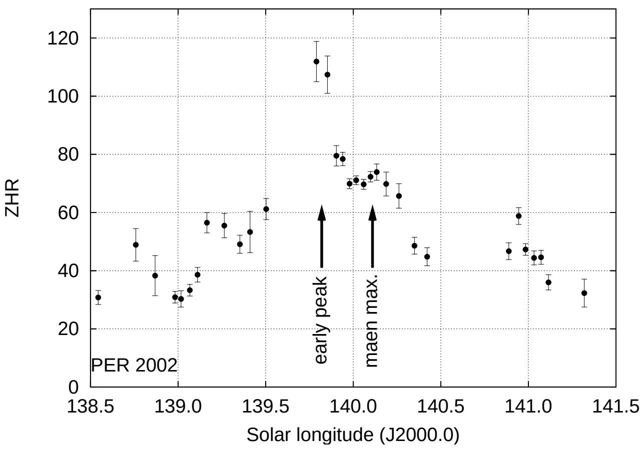

Figure 6 – The 2002 maximum period shows high ZHRs before the mean maximum occurs. We used the r-profile shown in Figure 5.

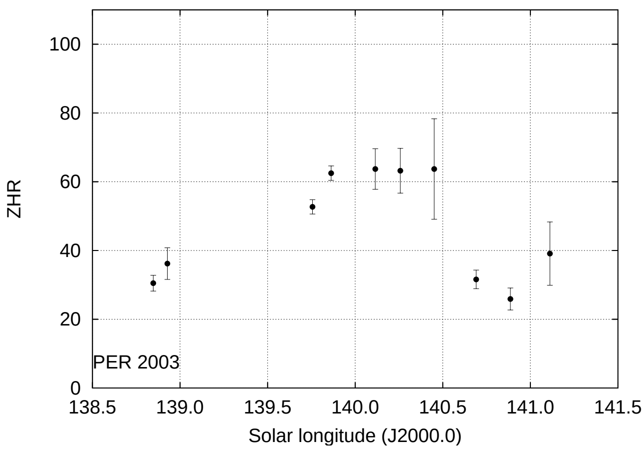

Figure 8 – The ZHR-profile of the 2003 Perseids shows a broad mean maximum. The ZHRs are calculated with the high r-values shown in Figure 7. Applying the standard values of r the maximum ZHRs had been below 60.

any deviation of the population index at the respective position, the density and flux also rise by about 50% over the usual figures of a Perseid maximum.

3.4 Smooth profiles in moonlit 2003 peak

This was another return of the Perseids with essentially the full moon coinciding with the Perseid maximum. Hence the amount of optical data is small. Contrary to the previous returns it seems that the population index r is higher than in moonless years (Figure 7), except for the period after the maximum. There is little chance to check whether this is an artefact due to the observing conditions (LM often $m = 5.5$ to 5.8). Nevertheless, the maximum ZHR is lower than usual, reaching a level of 65 for about $0\overset{\circ}{.}5$ in Solar longitude (Figure 8). Structures such as additional peaks are not detectable.

3.5 Four-revolution dust trail peak 2004

After the disappearance of the filament peak after the 1999 return, the perseids seemed to become less interesting. However, model calculations were presented at different occasions over the following years, indicating that peculiar features may become observable. The 2004 Perseids with no lunar interference brought the first occasion: Lyytinen and Van Flandern (2004) predicted the passage of the Earth through the 4-revolution dust trail of 109P/Swift-Tuttle on 2004 August 11, $20^{\rm h}50^{\rm m}$ UT, i.e. $\lambda_\odot = 139\overset{\circ}{.}440$. In various reports (Arlt, 2004; Berinde et al., 2004; Dubietis, 2004; Kac, 2004; Miskotte and Johannink, 2004; Trigo-Rodriguez et al., 2005) impressions or analyses of smaller data samples have been published, while the global data collected in the IMO's VMDB has not been analysed. Because of the size of the total sample, we used bins of $0\overset{\circ}{.}04$ shifted by $0\overset{\circ}{.}02$ between $139\overset{\circ}{.}4$ and $139\overset{\circ}{.}7$ for the ZHR graph. Even these short bins contained 1000 to 3400 Perseids each, except the last bin (582 Perseids at $139\overset{\circ}{.}654$).

The population index profile (Figure 9), also calculated with short bins ($0\overset{\circ}{.}1$ shifted by $0\overset{\circ}{.}05$ between $139\overset{\circ}{.}4$ and $139\overset{\circ}{.}7$) shows a local maximum of $r = 2.05 \pm 0.02$ at $\lambda_\odot = 139\overset{\circ}{.}43$, coinciding almost exactly with the position of the short-lived ZHR peak with ZHR $= 160 \pm 3$ at $\lambda_\odot = 139\overset{\circ}{.}450$ (Figure 10). This indicates the passage through the 4-revolution dust trail which seems to be composed of a higher portion of fainter meteors. The deviation between the predicted and the observed peaks is $0\overset{\circ}{.}01$ or less (seen the two high ZHRs in the profile), that is 15 minutes. The profile of the mean

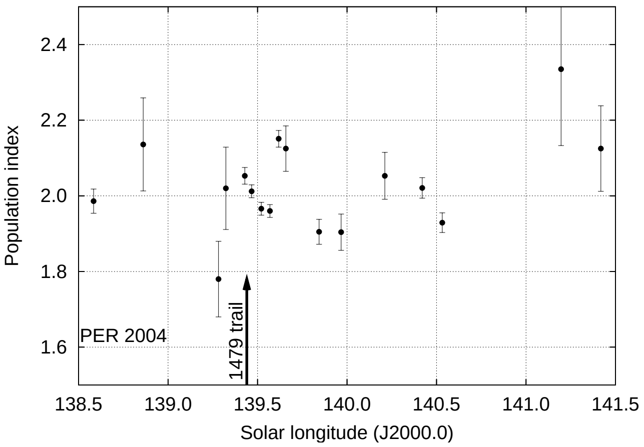

Figure 9 – Population index profile of the Perseids 2004. At the position of the 4-revolution dust trail the r-profile has a local maximum.

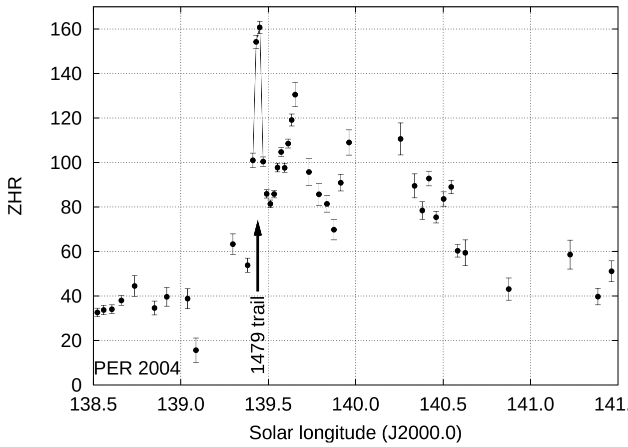

Figure 10 – The 2004 ZHR-profile based on the r-Profile shown in Figure 9 shows the peak of the 4-revolution dust trail very close to the position calculated by Lyytinen and Van Flandern (2004). Another peak occurs at $139\overset{\circ}{.}654$.

maximum yields a ZHR of about 75 during the trail peak. So the peak component itself provides a ZHR of about 85. Hence the observable population is composed of about 50% each from the mean maximum and the trail. As discussed earlier, the slightly higher value of the population index r over the average mean maximum profile indicates that the trail particles yield an even higher value of r. Therefore the number density (of particles causing meteors of at least $m = +6.5$) and flux, which depend sensitively on the value of r, are higher than in the mean stream.

Another ZHR-peak of 130 ± 5 at $139\overset{\circ}{.}654$ could be associated at a first glance with the peak in the population index at the same position. However, the average limiting magnitudes in this period are very close to $m = +6.5$, and therefore the ZHR is essentially independent of the value of the population index. Consequently, we should regard the peak as a true structure in the 2004 passage through the Perseid meteoroid stream, increasing the ZHR from about 85 (in the mean maximum profile) to 130. That is an increase by about 50%, again coinciding with a higher r and thus a significant density increase in the stream.

The mean rate maximum is less covered with data. The profile (Figure 10) shows ZHRs of 110 at $139\overset{\circ}{.}96$ as well as $140\overset{\circ}{.}25$, so that the assumption of a mean peak near the usual location of $140\overset{\circ}{.}1$ is reasonable. Nevertheless, the rate is well above the average of the 2000–2003 returns.

3.6 Many predictions for 2005

After the 2004 peak many observers became alert about the Perseids. In 2005, information about trail encounters and the mean maximum conditions were distributed mainly over the internet. Via the `meteorobs` mailing list, Esko Lyytinen mentioned another encounter of the 4-revolution trail (meteoroids released in 1479 AD) on 2005 August 12, about $09^{\rm h}$ UT at $\lambda_\odot = 139\overset{\circ}{.}68$ (message written on 2004 June 1). In the same mailing list, Mikhail Maslov refers to similar calculations of Isao Sato and his own raw calculations. There was an approach to the stream, but the chances for enhanced rates were considered to remain low (message written on 2004 December 2). Mikiya Sato added his result for 2005 also via the `meteorobs` mailing list on December 3, indicating an encounter on 2005 August 12, $08^{\rm h}57^{\rm m}$ UT at $\lambda_\odot = 139\overset{\circ}{.}681$, pointing out that there will be no enhanced rate. The mean maximum was calculated for 2005 August 12, $03^{\rm h}54^{\rm m}$ UT at $\lambda_\odot = 139\overset{\circ}{.}478$ by Vaubaillon at `www.imcce.fr/fr/ephemerides/phenomenes/meteor/PER/2005Perseids.php`. This is a relatively early position given the average longitude of the mean maximum.

The population index r is between 1.9 and 2.0 over most of the period (Figure 11). However, there are two minima: $r = 1.73 \pm 0.03$ at $\lambda_\odot = 139\overset{\circ}{.}67$, and $r = 1.67 \pm 0.06$ at $\lambda_\odot = 140\overset{\circ}{.}69$. Details about the bin lengths for the r-profile are listed in Table 3. The minima of the population index do not coincide with structures in the ZHR profile (Figure 12). The arrows in Figure 12 refer to the predicted positions of the mean maximum and the 4-revolution dust trail (with no expected activity).

The first ZHR peak at $\lambda_\odot = 139\overset{\circ}{.}38$ is about $0\overset{\circ}{.}1$ or 2.5 hours before Vaubaillon's predicted position. Actually the highest peak occurs at $\lambda_\odot = 139\overset{\circ}{.}75$ which is close to the position of the 1479 dust. One could suspect the mean maximum position at $140\overset{\circ}{.}2$. Considering that the periods $139\overset{\circ}{.}1$ – $139\overset{\circ}{.}5$ as well as $140\overset{\circ}{.}1$ – $140\overset{\circ}{.}5$ are best covered with data, we could also assume a broad maximum for which a parabolic fit would yield a maximum position of about $139\overset{\circ}{.}8 \pm 0.2$.

Combining the information of both the r and ZHR profiles, the appropriate interpretation is that we see traces of the 4-revolution dust trail at $\lambda_\odot = 139\overset{\circ}{.}75$ (predicted $139\overset{\circ}{.}68$) superposed on a broad mean Perseid maximum centered near $139\overset{\circ}{.}8 \pm 0.2$.

3.7 Smooth profiles in 2006

This was another return with a waning gibbous moon essentially disturbing the entire portion of the night with reasonably high Perseid radiant position around the maximum. Hence the sample remained small. The population index profile (Figure 13) shows a similarity to the moonlit 2003 return (Figure 7): the minimum values of r are 2.0 which is again higher than the aver-

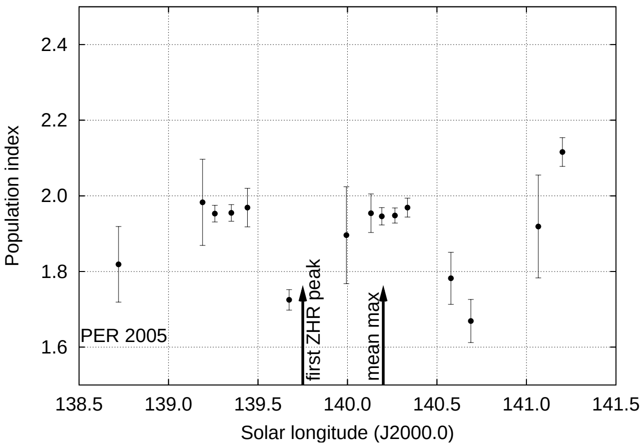

Figure 11 – Population index profile of the Perseids 2005. Arrows mark the predicted positions of the early and the mean ZHR-maximum found in our data.

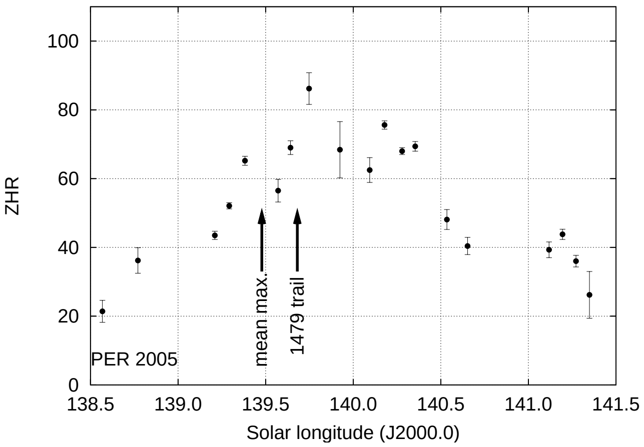

Figure 12 – ZHR-profile of the 2005 Perseids based on the r-Profile shown in Figure 11. Arrows show the predicted positions of an (early) mean maximum (Vaubaillon) and the encounter of the 1479 dust trail (Lyytinen and Sato; see text for details).

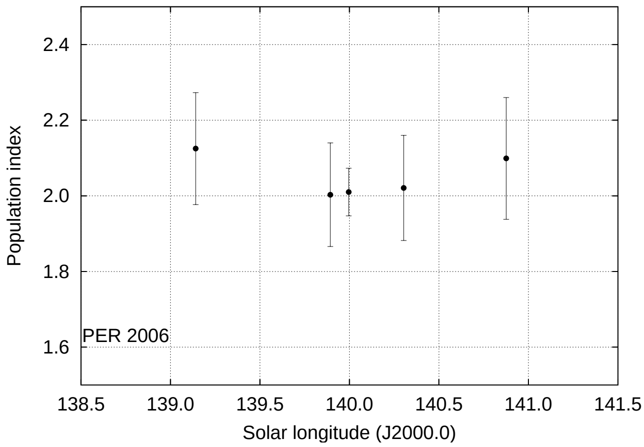

Figure 13 – The amount of available data does not allow the calculation of a detailed population index profile of the Perseids in 2006. The values do not deviate from the standard $r \approx 2$.

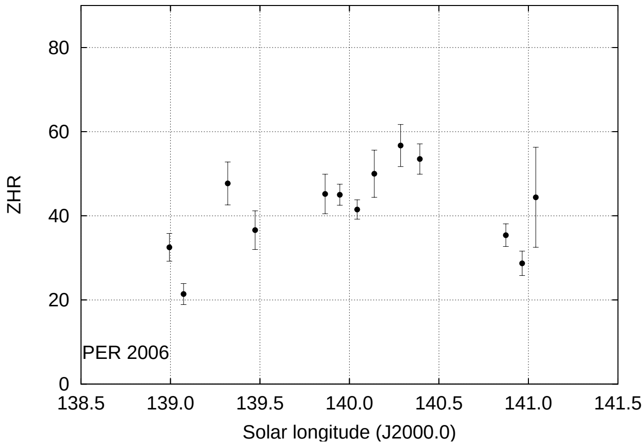

Figure 14 – Profile of the ZHR for the Perseids 2006 based on the r-Profile shown in Figure 13.

age for the interval shown here. Also like in 2003, the maximum ZHRs (Figure 14) are well below the average of the other returns of the 2000–2007 period. The highest value of 57 ± 5 at $\lambda_\odot = 140.^\circ 3$ is part of the mean maximum profile which is at the average position found for the given period.

3.8 Dust trail plus resonant Perseids in 2007

On 2007 August 5, Jenniskens et al. published a note in the Central Bureau Electronic Telegram number 1019. The authors provided information about different peaks for the 2007 return: the mean maximum should occur at $\lambda_\odot = 140.^\circ 196$ (August 13, 10^h UT). Furthermore, the 4-revolution dust trail was expected to produce enhanced rates on August 12/13, with peak times of 22^h42^m UT ($139.^\circ 754$; Vaubaillon), 22^h55^m UT ($139.^\circ 755$; Sato) or 00^h27^m UT ($139.^\circ 815$; Lyytinen), respectively. Particles trapped in a mean-motion resonance with Jupiter should add to the activity analogous to the 1989–97 returns with a ZHR of about 20 on August 13, 04^h UT ($139.^\circ 956$; Jenniskens).

In order to obtain information about the three peaks and their possibly different particle population, we calculated a population index profile with high temporal resolution (Figure 16). The bins were $0.^\circ 08$ shifted by $0.^\circ 04$ (1 hour) in the interval $\lambda_\odot = 139.^\circ 1 - 140.^\circ 1$. However, the values of r in these short intervals seem to produce only scatter and no clear structures. So the chance to identify one of the three features indicated by arrows by a deviating r is small. Of course, the smoother profile (Figure 15) with $0.^\circ 4$ shifted by $0.^\circ 2$ (5 hours) smears out all details. Both seem vaguely to indicate a higher $r \approx 2.1$ near the 1479 dust and the resonant Perseids and a lower $r \approx 1.9$ near the mean maximum.

Again, as in 2004 the limiting magnitudes in this period are mainly in the range 6.2–6.6 and therefore the ZHR depends only slightly on the r-value. So the ZHR profile (Figure 17) is almost independent of the applied r-Profile.

Therefore, we can try to identify features in the ZHR graph. The mean maximum is obviously situated at $140.^\circ 2$ (also marked by a minimum r). This confirms the average position over the last decade as well as the value given by Jenniskens.

The resonant Perseids could be dominating at $139.^\circ 92$ with the highest ZHR $= 88 \pm 6$ (of course being a superposition of the mean maximum and resonant meteoroids). Considering a smooth mean maximum ZHR

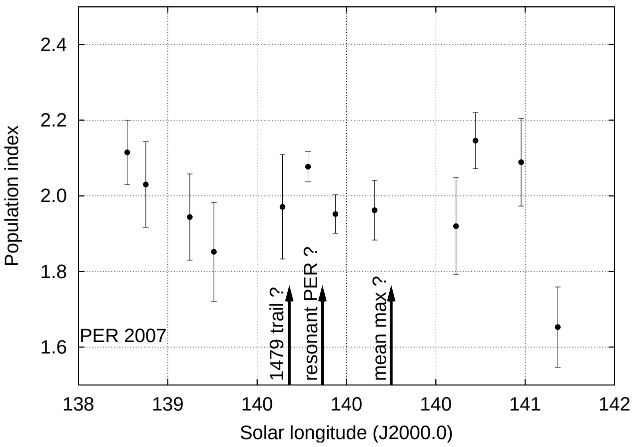

Figure 15 – Population index profile of the Perseids 2007 with low resolution. At the predicted trail, filament and mean maximum positions no obvious r-features can be found.

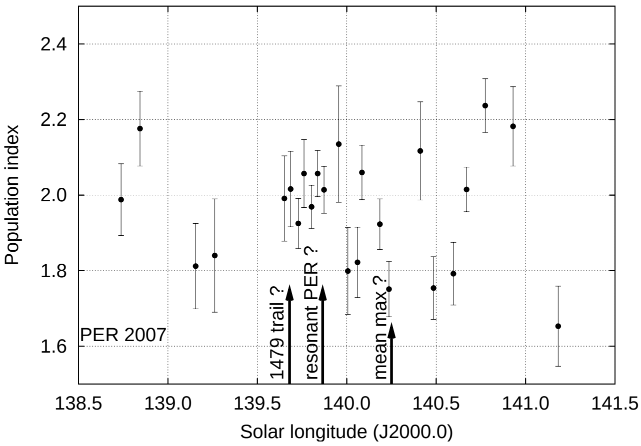

Figure 16 – Higher resolution population index profile of the 2007 Perseids. While the mean maximum position coincides with a minimum r, the other two peaks are difficult to combine with features in the r-profile.

profile — which is quite difficult — we may estimate the additional contribution of the resonant meteoroids to be nearly 50% of the normal rate. The difference to the predicted position is less than $0\overset{\circ}{.}04$ (1 hour). The population index shows no signature at either position.

Unfortunately there is a gap in the data before $139\overset{\circ}{.}65$. Thus it is not clear whether the first ZHR after the gap indeed is a maximum or just part of a peak which is located slightly earlier, which possibly can be identified with the passage through the 1479 dust trail. If so, the difference between the observed and calculated positions is $0\overset{\circ}{.}15$ (almost 4 hours). The population index (Figures 15 and 16) does not show peculiarities here.

4 Discussion

Given the model calculations and the given observation circumstances, the data of the 2004, 2005, and 2007 returns were of special interest.

The mean Perseid maximum regularly occurs at $\lambda_\odot = 140\overset{\circ}{.}1$. In most cases this period shows a lower population index r than the average of the period $\lambda_\odot = 138\overset{\circ}{.}5 - 141\overset{\circ}{.}5$. Data from two returns which were badly affected by moonlight (2003, 2006) yield a value

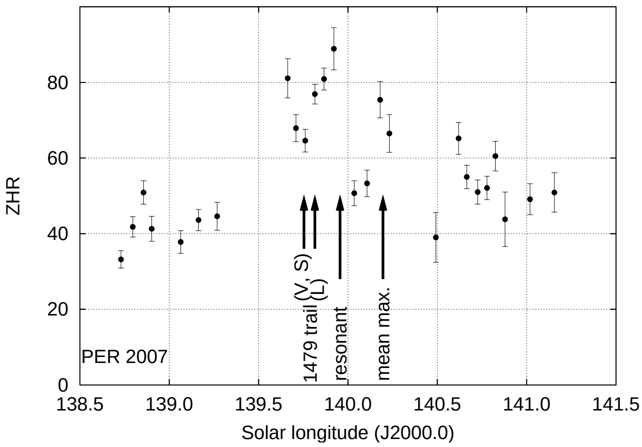

Figure 17 – In the ZHR-profile of the 2007 return (based on the r-Profile shown in Figure 16) we may identify three peaks: the mean maximum and the resonant meteoroids are close to their predicted positions (arrows). Traces of the 1479 trail may be the reason for the higher ZHRs about $0\overset{\circ}{.}15$ before the predicted position (V–Vaubaillon; L, S–Lyytinen and Sato).

of $r \approx 2.0 - 2.2$ which is higher than the usual $r \approx 1.8 - 1.9$. However, this is not the case in 2000 which was also observed with bad moonlight interference.

Peaks of the 4-revolution dust trail (meteoroids released in 1479 AD from comet 109P/Swift-Tuttle) can be found in 2004 (strongly), 2005 (weakly) and probably in 2007. The difference between the calculated and the observed position could be due to the fact that the Earth crossed outer regions of the trail in 2007.

The 2007 Perseids also showed meteoroids trapped in orbits resonant with Jupiter. Table 4 summarizes the data of the present analysis as well as the results from the 1988–1999 period when the filament meteoroids provided strong outbursts.

The average position of the mean maximum derived from the 2000–2007 data is $\lambda_\odot = 140\overset{\circ}{.}11 \pm 0\overset{\circ}{.}10$ with a ZHR of 77 ± 12. Omitting the data from returns affected by bright moonlight (2000, 2003, and 2006), the average is $\lambda_\odot = 140\overset{\circ}{.}10 \pm 0\overset{\circ}{.}08$ and the average ZHR is then 81 ± 8. Including data of all 20 returns listed in Table 4, we obtain $\lambda_\odot = 140\overset{\circ}{.}06 \pm 0\overset{\circ}{.}12$ and a ZHR of 84 ± 10.

5 Conclusions

Global visual data of the Perseid returns allow us to detect the mean maximum of the stream as well as various features caused by the Earth's passage through filaments, dust trails and regions of resonant meteoroids (2007).

Encounters with the 4-revolution dust trail of 109P/Swift-Tuttle were detected in 2004 (strongly), 2005 (weakly) and 2007 (probably). Differences between the predicted and observed center passages were 1 hour or less in 2004 and 2005, but larger in 2007. This may indicate that the Earth crossed just the outer edge of the trail.

Predictions of future trail encounters provide the opportunity to test the stream models. The analysis also emphasizes that global visual observational data is adequate to obtain annual profiles of the population index r

Table 4 – The mean Perseid maximum with a ZHR in the range between 60 and about 115 occurs at $\lambda_\odot = 140\overset{\circ}{.}1 \pm 0\overset{\circ}{.}1$ (J2000). Additional peaks related to dust trails or stream filaments have been observed in many years. Positions and peak ZHRs are summarized below.

Year	Mean maximum $\lambda_\odot$	Mean maximum ZHR_{max}	Filament peak $\lambda_\odot$	Filament peak ZHR_{max}	Reference and remarks
1988	140°.08±0°.04	106±22	139°.78±0°.03	86± 4	Roggemans, 1989; Brown & Rendtel, 1996
1989	139°.80±0°.09	94± 6	139°.56±0°.03	102±10	Koschack & Roggemans, 1991; Brown & Rendtel, 1996
1990	140°.54±0°.2	81±61	139°.55±0°.05	75±10	Brown & Rendtel, 1996
1991	139°.94±0°.04	97± 2	139°.55±0°.03	284±63	Brown & Rendtel, 1996
1992	140°.13±0°.2	84±34	139°.48±0°.02	220±22	Brown & Rendtel, 1996
1993	139°.91±0°.04	98± 5	139°.53±0°.01	264±17	Brown & Rendtel, 1996
1994	139°.84±0°.04	86± 2	139°.59±0°.01	238±17	Brown & Rendtel, 1996
1995	139°.90±0°.15	65±20	139°.62±0°.05	171±30	Rendtel & Arlt, 1996
1996	140°.08±0°.04	85±10	139°.66±0°.03	121±17	Rendtel & Arlt, 1996
1997	140°.03±0°.03	94± 2	139°.71±0°.01	137± 5	Arlt, 1998
1998	140°.10±0°.02	74± 3	139°.75±0°.03	110±20	Arlt, 1999
1999	139°.9 ±0°.02	87± 6	139°.80±0°.01	104± 4	Rendtel & Arlt, 1999
2000	139°.97±0°.02	97± 3	none	—	Arlt & Händel, 2000; this work
2001	139°.8 ±0°.2	71± 8	none	—	This work
2002	140°.11±0°.06	74± 3	139°.82±0°.04	110± 8	Arlt & Buchmann, 2002; this work
2003	140°.1 ±0°.2	64± 7	none	—	This work
2004	140°.15±0°.20	115±10	139°.44±0°.01	160± 4	This work
			139°.65±0°.05	130± 7	This work
2005	140°.2 ±0°.1	76± 3	139°.75±0°.05	86± 5	This work
2006	140°.29±0°.10	57± 7	none	—	This work
2007	140°.25±0°.05	67± 8	139°.65±0°.03	78± 5	Peak uncertain; this work
			139°.86±0°.03	88± 6	Resonant meteoroids; This work

and the ZHR. Observers should try to collect data also in the case of disturbing moonlight close to the peak periods of the Perseids (as well as other major showers) because a larger sample allows one to derive reliable information about the streams.

The average position of the mean maximum is $\lambda_\odot = 140\overset{\circ}{.}1 \pm 0\overset{\circ}{.}1$ with a ZHR of 77 ± 12. A larger sample from the 20 returns 1988–2007 essentially yields the same average. This also holds when data moonlight-affected returns (2000, 2003, and 2006) are excluded ($\lambda_\odot = 140\overset{\circ}{.}10 \pm 0\overset{\circ}{.}08$ and ZHR $= 81 \pm 8$.

Acknowledgements

We thank all observers who sent their data to the IMO's Visual Commission for inclusion in the Visual Meteor DataBase (VMDB).

References

Arlt R. (1998). "Global analysis of the 1997 Perseids". *WGN*, **26**, 61–71.

Arlt R. (1999). "Global analysis of the 1998 Perseid meteor shower". *WGN*, **27**, 237–249.

Arlt R. (2004). "Meteor shower analysis exemplified". In *Proceedings IMCVarna 2004*, pages 17–20.

Arlt R. and Buchmann A. (2002). "Global analysis of the 2002 Perseids". *WGN*, **30**, 232–243.

Arlt R. and Händel I. (2000). "The 'new' peak failed: first analysis of the 2000 Perseids". *WGN*, **28**, 166–171.

Berinde S., Conu A., and Grigore V. (2004). "Results of the Perseids-2004". In *Proceedings IMC Varna 2004*, pages 21–24.

Brown P. and Rendtel J. (1996). "The Perseid meteoroid stream: characterization of recent activity from visual observations". *Icarus*, **124**, 414–428.

Dubietis A. (2004). "The 2004 Perseid outburst from Lithuania". *WGN*, **32**, 129–130.

Jenniskens P. (2006). *Meteor showers and their parent comets*. Cambridge University Press, Cambridge, 790 pages.

Jenniskens P., Betlem H., de Lignie M., Ter Kuile C., van Vliet, M. C. A.AND van 't Leven J., Koop M., Morales E., and Rice T. (1998). "On the unusual activity of the Perseid meteor shower (1989–96) and the dust trail of comet 109P/Swift-Tuttle". *MNRAS*, **301**, 941–954.

Jenniskens P., Sato I., Lyytinen E., and Vaubaillon J. (2007). "Perseid meteors 2007". *Central Bureau Electronic Telegrams*, **1019**, Aug 05.

Kac J. (2004). "Perseids 2004 — observations by the MBK team". In *Proceedings IMC Varna 2004*, pages 52–57.

Koschack R. and Roggemans P. (1991). "The 1989 Perseid meteor stream". *WGN*, **19**, 87–98.

Lyytinen E. and Van Flandern T. (2004). "Perseid one-revolution outburst in 2004". *WGN*, **32**, 51–53.

Miskotte K. and Johannink C. (2004). "DMS results of the 2004 Perseids". *WGN*, **32**, 151–153.

Rendtel J. and Arlt R. (1996). "Perseids 1995 and 1996 — an analysis of global data". *WGN*, **24**, 141–147.

Rendtel J. and Arlt R. (1999). "First results of the 1999 Perseid meteor shower". *WGN*, **27**, 250–255.

Roggemans P. (1989). "The Perseid meteor stream in 1988: a double maximum". *WGN*, **17**, 127–137.

Trigo-Rodriguez J. M., Vaubaillon J., Ortiz J. L., Castro-Tirado A., Jelinek M., de Ugarte Postigo A., Santos Sanz P., Aceituno Castro F. J., Llorca J., Lyytinen E., Sanchez Caso A., Bernal Gonzalez A., Pastor Erades J., and Ocaña F. (2005). "Orbital elements of 2004 Perseid meteoroids perturbed by Jupiter". *Earth, Moon, Planets*, **97**, 269–278.

Bright Perseids in 2007

Andrey Murtazov [1,2], *Alexander Efimov* [3] *and Dmitry Kolosov* [4]

The results of the 2007 Bright Perseids observations using a wide-angle camera are presented.

Received 2008 March 3

1 Introduction

In 2007 July-August, we carried out optical monitoring of the circumterrestrial space pollution with the bright Perseid meteoroids.

The observations were conducted near Ryazan, Russia, $\lambda = 02^{\mathrm{h}}39^{\mathrm{m}}$, $\phi = 54g28'$.

2 Observations

The observations were performed using a Wat-902H camera and a Computar T2314FICS lens with a field of view $113^\circ\!.3 \times 86^\circ\!.3$ (like Yrjölä, 2003) that was directed towards the local zenith. The control and registration were provided using a Pinnacle Media Center EN as a grabber and an AMD Turion 64 Mobile processor, 1.60 GHz, 1 Gb RAM.

The equipment functioned in the mode assigned for registering bright meteors that constitute a danger for space hardware operating in the circumterrestrial space (Murtazov et al., 2007). Figure 1 shows the brightness distribution of meteors observed on 2007 August 7-13. It also presents a theoretical curve of the Perseid magnitudes which corresponds to their population index ($r = 2.6$), normalised to $N = 1$ at $m = -3$.

The bright Perseid observation results are provided in Table 1.

They show that the bright meteor time distribution is quite irregular and has rather a broad stream maximum. The stream intensity near the maximum grows rather rapidly, as on August 7/8 the number of Perseids was slightly higher than their total number observed in late June and after twenty four hours it grew almost two-fold. The share of bight meteors not related to the Perseids in the total number of registered ones accounted for: 11.5% on August 11/12 and 13.8% on August 13/14, but they were absent on August 7/8.

The key stream parameters were calculated as follows.

The stream density is

$$\Phi = \frac{N \sin(h)}{7.2 \times 10^3 H^2 \tan A \tan B} \quad [\mathrm{km}^{-2}\mathrm{s}^{-1}] \qquad (1)$$

where N [hour^{-1}] is the HR of the observable meteors with semi-angle dimensions $A \times B$ [arc degree]; h is the angular altitude of the shower radiant; and H [km] is the meteor burning height.

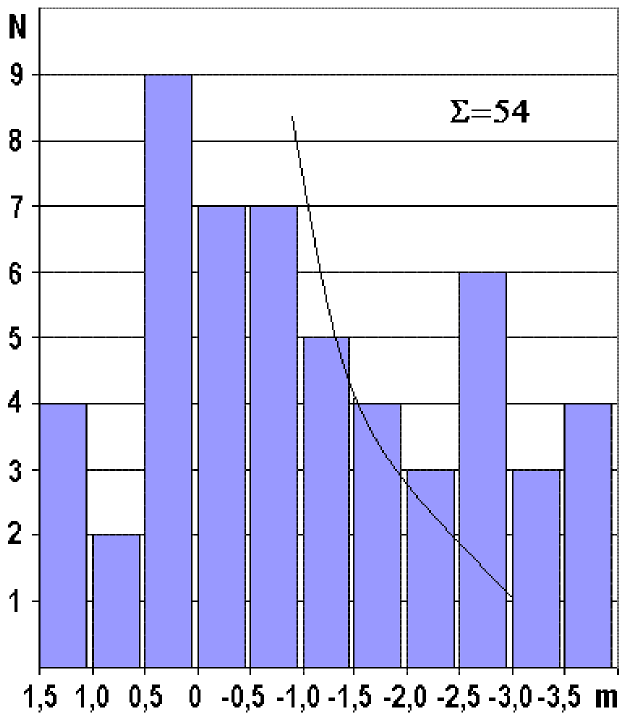

Figure 1 – Wat-902H Perseid Magnitude Distribution, 2007 August 7-13

Stream spatial density:

$$D = \frac{\Phi}{v} \quad [\mathrm{km}^{-3}] \qquad (2)$$

where v [km/s] is the meteor stream velocity.

For the Perseid meteors these are $H = 100$ km, $v = 60$ km/s.

The average values of the bright meteoroids' spatial density per observation night of 2007 July–August are show in Figure 2. They were obtained from averaging hour rates with regard to changes of the shower radiant angular altitude at this time. The data of the August 13/14 night (dashed line) are valued based on visual observations. The figure also presents the maxima of the main meteor streams of the related period.

3 Conclusion

We conclude that the space density of dangerous meteoroids in Perseids in 2007 was very low. For instance, in 2002 the hour rates of bright Perseids were about a hundred times as much as in 2007 with $D = (1.3 - 3.0) \times 10^{-8}$ km^{-3} (Murtazov, 2004).

[1] The Ryazan State University, Astronomical Observatory. E-mail: a.murtazov@rsu.edu.ru
[2] Ap. 11, 72/76, Zatynnaya St., Ryazan, 390006, Russia.
[3] Ap. 22, 26, Ostrovskogo St., Ryazan, 390035, Russia.
[4] Ap. 51, 39/1, Moskovskoe Shosse St., Ryazan, 390044, Russia.

IMO bibcode WGN-364-murtazov-perseids
NASA-ADS bibcode 2008JIMO...36...77M

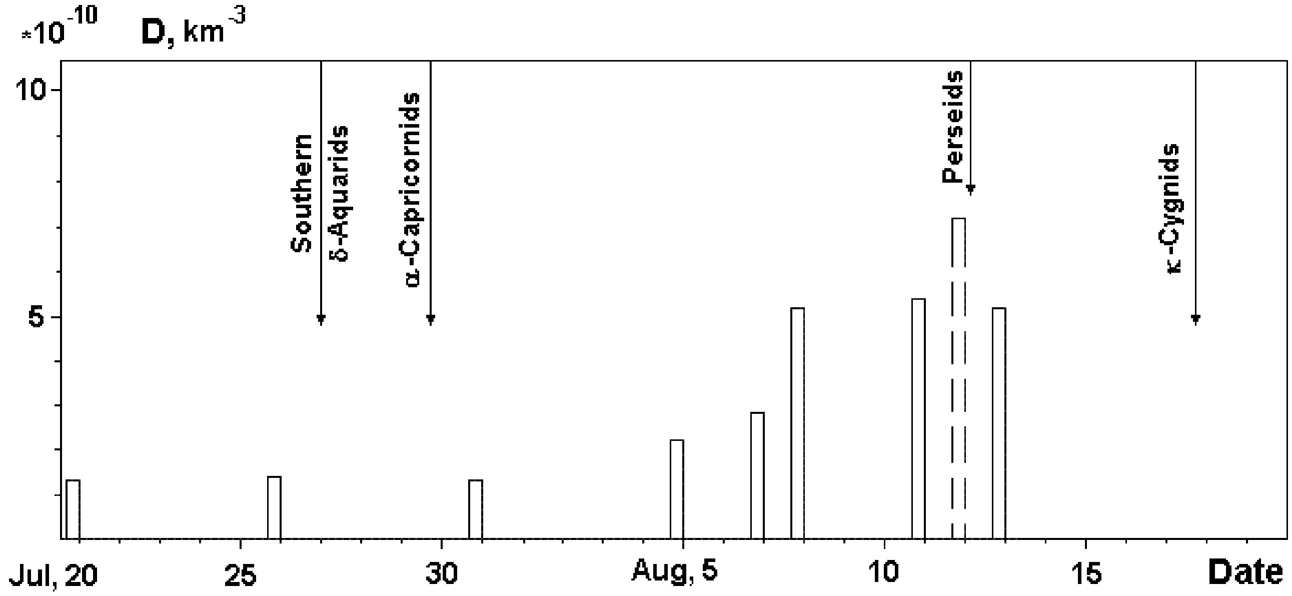

Figure 2 – Spatial Density of Bright Perseids in July-August, 2007.

Table 1 – Number of Bright Perseids in 2007 August.

Date	Time Interval, UTC (h, m)	Solar Longitude Interval (arc degrees)	Number of bright meteors
2007 August 07	19^h00^m–20^h00^m	134°.902–134°.942	2
	20^h00^m–21^h00^m	134°.942–134°.982	2
	21^h00^m–22^h00^m	134°.982–135°.021	2
	22^h00^m–23^h00^m	135°.021–135°.061	4
	23^h00^m–24^h00^m	135°.061–135°.102	2
2007 August 08	19^h00^m–20^h00^m	135°.861–135°.901	4
	20^h00^m–21^h00^m	135°.901–135°.941	6
	21^h00^m–22^h00^m	135°.941–135°.981	5
	22^h00^m–23^h00^m	135°.981–136°.020	4
	23^h00^m–24^h00^m	136°.020–136°.060	4
2007 August 11	19^h00^m–20^h00^m	138°.739–138°.779	1
	20^h00^m–21^h00^m	138°.779–138°.819	0
	21^h00^m–22^h00^m	138°.819–138°.859	8
	22^h00^m–23^h00^m	138°.859–138°.899	5
	23^h00^m–24^h00^m	138°.899–138°.938	9
2007 August 13	19^h00^m–20^h00^m	140°.659–140°.699	10
	20^h00^m–21^h00^m	140°.699–140°.739	4
	21^h00^m–22^h00^m	140°.739–140°.779	2
	22^h00^m–23^h00^m	140°.779–140°.819	4
	23^h00^m–24^h00^m	140°.819–140°.859	4

References

Murtazov A. (2004). “Contamination of circumterrestrial space during meteor showers”. In *Near-Earth Astronomy-2003, V. 1. Proceedings of the conference*, pages 248–251. Russian Academy of sciences institurte for astronomy. St. Petersburg. VVM Co. Ltd.

Murtazov A., Voskresensky A., Kolosov D., and Titov P. (2007). “Ecological optical monitoring of circumterrestrial space pollution”. *Ecological Systems and Equipment*, **3**, 24–26.

Yrjölä I. (2003). “Meteor video camera”. `www.kolumbus.fi/oh5iy/astro/ Ccd.html` . Nov. 2003.

Ongoing meteor work

Comparison of TV magnitudes and visual magnitudes of meteors

Yoshihiko Shigeno [1] *and Masayuki Toda*

The generally accepted belief is that a meteor, with a large amount of infrared rays, can be captured brighter than it actually is by infrared-sensitive image intensifiers (I.I.) or CCD. We conducted observations of meteors using three methodologies: 1) I.I. with an attached filter that has the same spectral response as the human eye at night vision, 2) I.I. without the filter and 3) visually to determine meteor magnitudes. A total of 31 members of the astronomical club at Meiji University observed 50 Perseid meteors, 19 Geminid meteors as well as 44 sporadic meteors and the results were tabulated. The results helped us understand that on average I.I. can record meteors as brighter than visual observation by the magnitude equivalent of 0.5 for Perseids, 1.0 for Geminids and 0.5 for sporadic meteors.

For I.I. with a filter that has the same spectral response the human eye at night vision, it turned out that we could obtain almost the same magnitude with observation by the human eye.

We learned that a bright meteor with negative magnitude can be observed by I.I. brighter than the human eye. From several examples, we found I.I. could record a meteor with about −1 visual magnitude as brighter by about three magnitudes. We could probably do so because a bright meteor with negative magnitude may contain more infrared rays and the brightness could be amplified.

Received 2008 June 6

1 Introduction

Magnitudes are important yardsticks to express the mass of meteoric materials and conventionally visual magnitude or photographic magnitude have been used as the index (Öpic, 1958; Verniani, 1967). Since a meteor contains more infrared rays (Borovička et al., 1999), the generally accepted belief is that meteors can look brighter when photographed by new observation instruments such as I.I. or CCD with more sensitivity to infrared rays. By obtaining precisely the difference between conventional and new magnitudes of the same meteors, we are able to compare the conventional and new observation in a correct manner. However, it appears that this comparison has not yet been implemented in a full scale. We would like to report the results of the comparison of I.I. and visual observations.

2 Comparison between TV magnitudes and visual magnitudes

Shigeno and Toda conducted a series of observations to determine meteor magnitudes by both I.I. and visual observations: once in April and twice in August 2004. During the observations, we found a total of 21 meteors; for each meteor, its TV magnitudes were brighter than visual magnitude by 0.2 to 2.6 magnitude or 1.2 magnitude on average. It will be attributed to I.I. that is also sensitive to infrared rays and capture brighter image of meteors as they contain more infrared rays.

We studied whether the difference between TV magnitudes and visual magnitudes ($m_{\rm tv} - m_{\rm v}$) could be changed or not by other factors. Figure 2 shows the relation between visual magnitude ($m_{\rm v}$), angular velocity (Va) and observed velocity (VO) where the trend is not clear yet (Shigeno & Toda, 2005).

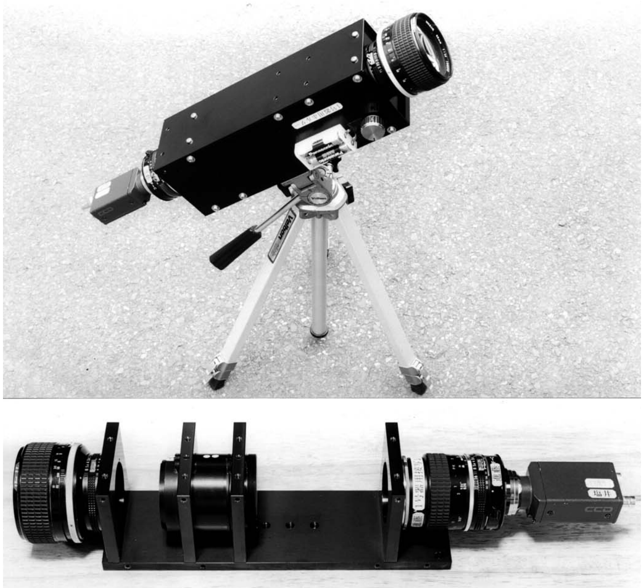

Figure 1 – The TV observation equipment. The device with the Image Intensifier (Delft High Tech XX1470 etc.).

3 Observation by I.I. with filter for spectral response equivalent of visual magnitude

The above observation method cannot determine the correct visual magnitude. We, therefore, observed to determine meteor magnitudes by three other methods: 1) I.I. with a filter that has the same spectral response as visual magnitude at night vision ($m_{\rm tvF}$), 2) I.I. without the filter ($m_{\rm tv}$) and 3) visually. Magnitudes of TV meteors were obtained from the relations between brightness, size and magnitudes of fixed stars and corrected

[1] 5–6 Kizuki-Sumiyoshi, Kawasaki City, 211-0021, Japan. Email: cyg@nikon.co.jp

IMO bibcode WGN-364-shigeno-magnitudes
NASA-ADS bibcode 2008JIMO...36...79S

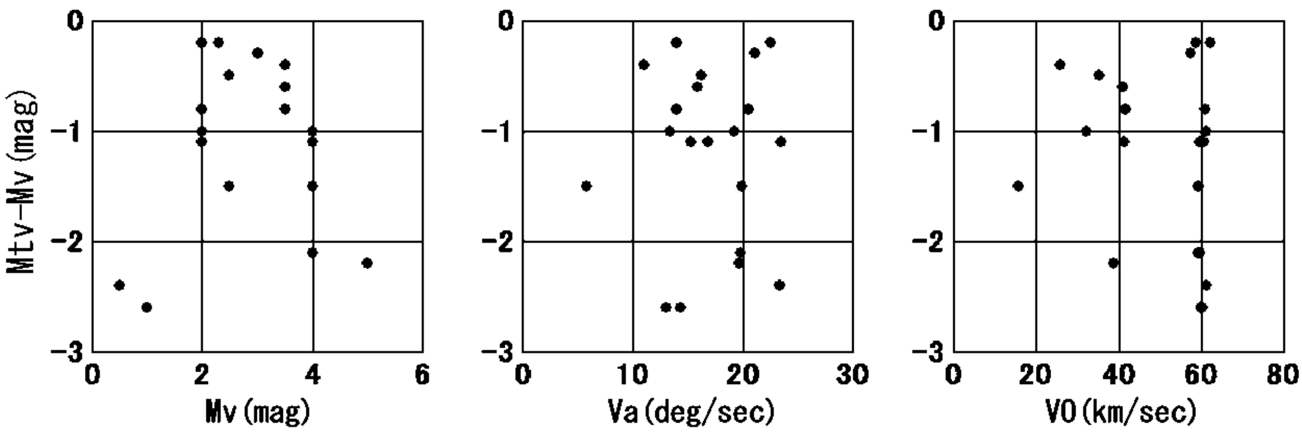

Figure 2 – Comparison between deviation (TV magnitude − Visual magnitude) ($m_{tv} - m_v$) and Visual magnitude (m_v), Angular velocity (Va), Observed velocity (VO).

Table 1 – Tabulations by observers for comparison of magnitudes by I.I. and visual observation. $m_{tv} - m_{tvF}$: Comparison of magnitudes without a filter (m_{tv}) and with a filter (m_{tvF}). $m_v - m_{tvF}$: Comparison of Visual magnitudes (m_v) and magnitudes with a filter (m_{tvF}).

Perseids				Geminids				Sporadic			
Observer	No.	Mean	SD	Observer	No.	Mean	SD	Observer	No.	Mean	SD
$m_{tv} - m_{tvF}$	50	-0.5	0.7	$m_{tv} - m_{tvF}$	19	-1.0	0.6	$m_{tv} - m_{tvF}$	44	-0.5	0.6
$m_v - m_{tvF}$				$m_v - m_{tvF}$				$m_v - m_{tvF}$			
Hosogi	2	-1.4	0.4	Sato	3	-0.9	1.2	Sakaguchi	1	-1.4	0.0
Yamashita	2	-0.9	0.3	Hirota	2	-0.7	0.6	Saito.Y	3	-1.1	0.4
Katabami	2	-0.7	0.1	Oshima	3	-0.5	1.6	Saito.S	1	-1.1	0.0
Kitagawa	1	-0.5	0.0	Arai	1	-0.4	0.0	Katabami	2	-1.0	0.5
Okuyama	3	-0.3	0.9	Kanaya	4	-0.3	0.7	Yamada	2	-0.6	0.8
Sakaguchi	2	-0.3	0.7	Yamashita	2	-0.2	0.3	Iino	2	-0.6	1.3
Shinsha	2	-0.3	0.4	Ogawa.H	2	-0.2	0.3	Sato	8	-0.5	0.9
Kinoshita	13	-0.3	0.7	Yuriya	2	-0.2	1.0	Okuyama	2	-0.4	0.1
Yuriya	18	-0.3	0.6	Matsuzaki	1	0.0	0.0	Kitamura	5	-0.4	0.5
Sato	9	-0.2	0.6	Kinoshita	6	0.0	0.9	Kanaya	12	-0.3	0.7
Wakasa	10	-0.2	0.6	Wakasa	4	0.2	1.1	Kinoshita	9	-0.2	1.0
Ogawa.Y	21	-0.2	0.8	Ogawa.Y	9	0.3	0.8	Kato.T	7	-0.1	0.7
Matsuzaki	3	-0.2	1.4	Shigeno	3	0.5	0.6	Ogawa.Y	15	-0.1	0.9
Doi	3	-0.2	0.3	Matsuda	5	0.5	0.7	Matsuda	4	-0.1	0.7
Kanaya	7	-0.1	0.7	Kitamura	5	0.7	0.9	Oshima	7	-0.1	0.7
Saito.Y	3	-0.1	0.5	Yamada	2	0.8	0.8	Yuriya	21	-0.1	0.5
Noto	4	-0.1	1.7	Saito.Y	3	1.7	0.7	Matsuzaki	4	0.0	0.5
Arai	20	0.0	0.8					Arai	11	0.1	0.6
Iino	8	0.0	1.0					Wakasa	9	0.1	0.6
Kato.T	2	0.1	1.0					Yamashita	3	0.2	0.3
Oshima	8	0.1	0.7					Doi	3	0.3	0.6
Kato.S	2	0.2	0.9					Kurosaki	4	0.4	0.4
Kurosaki	3	0.5	0.4					Toda	9	0.5	0.9
Hirota	3	0.6	1.0					Kato.S	1	0.6	0.0
Toda	13	0.7	1.1					Hirota	2	0.6	0.2
Shigeno	17	1.0	0.7					Hosogi	2	0.9	0.8
Kitamura	2	1.2	0.3					Shigeno	17	0.9	0.6
								Kitagawa	1	1.6	0.0
All Visual	183	0.0	0.9	All Visual	57	0.2	0.9	All Visual	167	0.0	0.8

for angular velocity. A total of 31 members of Meiji University's astronomical club observed 50 meteors in Perseids, from 2007 August 11 to August 13, 19 meteors in Geminids on December 14 of the same year and 44 sporadic meteors. The results are shown in Table 1 as tabulations by observers for comparison of magnitudes by I.I. and visual observation.

3.1 Comparison of m_{tv} with m_{tvF}

As shown by the upper row titled '$m_{\mathrm{tv}} - m_{\mathrm{tvF}}$' of Table 1, we obtained the following data: -0.5 magnitude for Perseids, -1.0 magnitude for Geminids and -0.5 magnitude for sporadic meteors. These results suggest that observation without filter shows brighter than observation with filter by 0.5 to 1.0 magnitude. In the table, SD indicates the dispersion of data as standard deviation and the results ranged from ± 0.6 to 0.7 magnitude, meaning they were the variation of data but not errors in the average values.

3.2 Comparison of m_{v} with m_{tvF}

The middle rows of Table 1 shows the tabulated results by observers. Negative values mean that the observers had estimated brighter than actual while positive values mean they had estimated darker. We learned that some observers had estimated brighter by almost one magnitude while others had estimated darker. However, from the total results of all the observers, i.e., 'All Visual Observation Data' in the bottom rows of Table 1, it turned out that the difference between the average of m_{v} and the average of m_{tvF} was somewhere between 0.0 to 0.2 magnitude and the difference was minimal. That means m_{tvF} in this report was almost meant to be m_{v}. However, we also learned data variation by the observers was rather large at ± 0.8 to 0.9 magnitude.

3.3 A bright meteor with negative magnitude

A bright meteor with negative magnitude can be recorded by I.I. brighter than visual observation. Figure 3 is a set of typical examples of meteors with negative magnitudes. They are classified as approximately -1 magnitude by visual observation whereas (1) m_{tvF} are brighter by approximately 1 magnitude and (2) m_{tv} are brighter by approximately 3 magnitudes.

We assume the reason for the above item 1 is due to the fact that the magnitude by TV observation is to determine the brightest spot instantaneously while visual observation determines averaged magnitude. Therefore, as a brighter meteor may likely generate more light instantaneously, TV observation may estimate the magnitude brighter than visual observation.

For the reason noted in item 2, we assume that brighter meteors with negative magnitude may be seen to be brighter as they may contain a large amount of infrared rays.

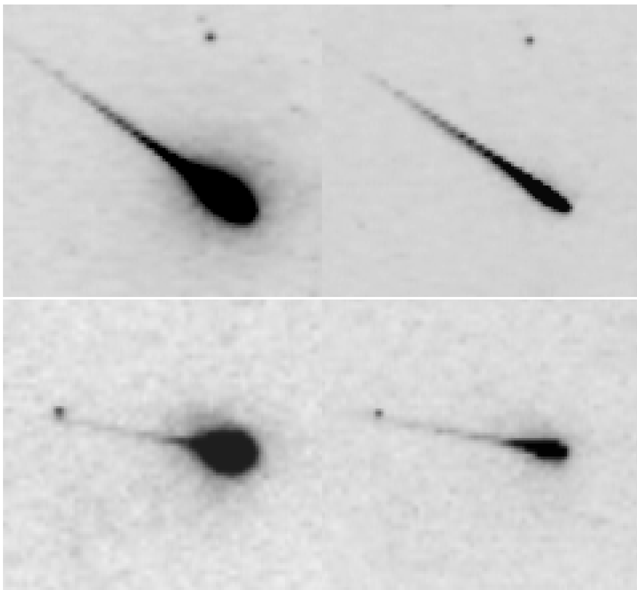

Figure 3 – Bright meteors with negative magnitude. Upper photo. : No.P40 Aug.12,2007 17:07:50(UT) Perseid. Upper left : $m_{\mathrm{tv}} = -4.0$. Upper right : $m_{\mathrm{tvF}} = -1.7$. $m_{\mathrm{v}} = -0.5$. Lower photo. : No.G05 Dec.14,2007 13:42:39(UT) Geminid. Lower left : $m_{\mathrm{tv}} = -4.8$. Lower right : $m_{\mathrm{tvF}} = -2.2$. $m_{\mathrm{v}} = -1.4$. Filter : SCHOTT BG18 2mm (Filter that has equivalent spectral response as the human eye at night vision (400 nm – 600 nm).) Spectrum sensitivity of I.I. : 350 nm – 900 nm.

4 Conclusion

Previous infrared spectrum observation of Perseids had discovered several molecular bands such as the 630–670 nm and 730–780 nm nitrogen molecular bands as well as many kinds of atomic luminescent lines such as the 777 nm oxygen atomic luminescent lines (Ebizuka, N., personal communication). We learned that these infrared rays make meteors look brighter by 0.5 to 1.0 magnitude; especially meteors of negative magnitudes can make the difference of brightness larger. Meanwhile, we also learned that I.I. with the filter that has the same spectral response as visual magnitude at night vision can observe meteors with almost identical magnitude of visual observation.

We would like to express our gratitude for valuable advice from Mr. Mitsuru Terada for the relations between magnitude and mass of meteors and from Mr. Noboru Ebizuka for the infrared spectrum.

5 Supplementary notes

We studied the relation between magnitudes and image sizes of fixed stars in order to precisely obtain magnitudes of meteors. Figure 4 shows the results of observations from two types of often-used objective lenses: $f = 85$ mm, $f/1.2$ and $f = 24$ mm, $f/1.4$, respectively. The relation between magnitudes of fixed stars darker than 0 magnitude and the size of image can be approximated into an almost straight line. However, we learned that fixed stars brighter than 0 magnitude may make the image size bigger rapidly. This would be because of the characteristics of I.I. Then, we chose straight-line approximation at an area darker than 0 magnitude while we used quadratic functional approximation at another area brighter than 0 magnitude in Figure 4 by

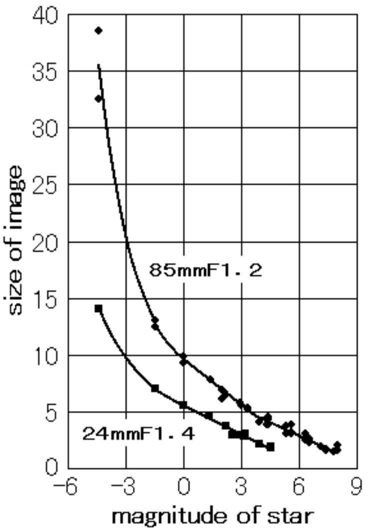

Figure 4 – Comparison between magnitude of star and size of image (mm diameter on a 17-inch monitor).

straight-line and curved line. Figure 4 shows the case of observation without the filter and the approximation is different in the case of observation with the filter.

Figure 5 shows a fireball discovered during TV observation of a Leonids meteor swarm in 2001 (Shigeno et al., 2003). The original data was recomputed by the methodologies in this report and the magnitude turned out to be $m_{\rm tv}$: −7.6. Unfortunately, however, we did not observe this meteor visually. That particular day happened to be a meteor storm occasion and a large number of people were observing but there was no report of such a bright meteor. The actual magnitude of visual observation of the meteor is assumed to be about −4 as there is a difference of approximately 3.5 magnitudes between $m_{\rm v}$ and $m_{\rm tv}$ as shown in Figure 3.

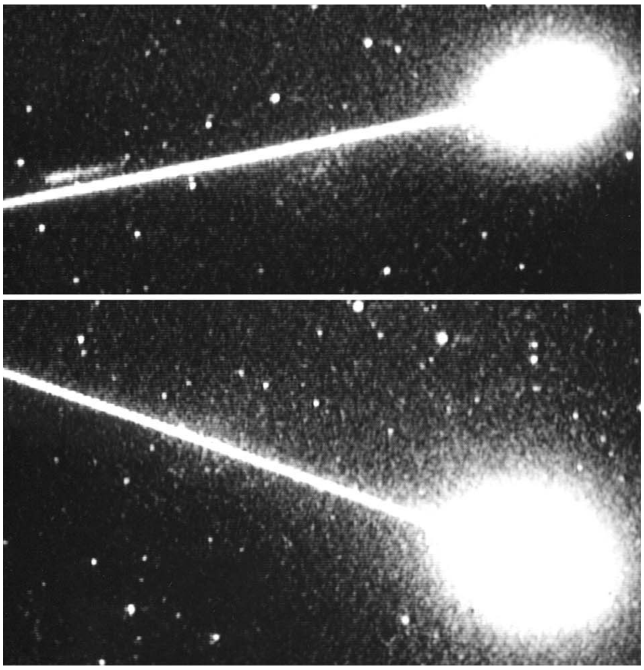

Figure 5 – An example of a double station TV meteor. ID: MSSJBZ on Nov 18 2001 at 18:19:34 (UT). TV magnitude ($m_{\rm tv}$) = −7.6.

References

Borovička J., Stork R., and Boček J. (1999). “First results from video spectroscopy of 1998 Leonid meteors”. *Meteoritics & Planetary Science*, **34**, 987–994.

Öpic E. J. (1958). *Physics of meteor flight in the atmosphere*. Interscience Publishers, Inc. Page 148.

Shigeno Y., Shioi H., and Shigeno T. (2003). “Radiants and orbits of the 2001 Leonids”. *The Institute of Space and Astronautical Science*, **SP 15**, 55–62.

Shigeno Y. and Toda M. (2005). “Double-station TV meteor observations (2004.08.11–12)”. *Nippon Meteor Society.*

Verniani F. (1967). “Meteor masses and luminosity”. *Smithsonian Contributions to Astrophysics*, **10**, 181–195.

All meteors have been made public at `http://www.imo.net/files/data/msswg/`

Meteoroid Environment Workshop and Call for Lunar Impact Observations

Rainer Arlt [1] *and Danielle Moser* [2]

In retrospect of a workshop held in Huntsville, Alabama, USA, we review the current contributions to the evaluation of the meteoroid environment in near-Earth space. We connect this report with a call for lunar impact observations which may be an interesting meteor project during the moon-disturbed hours of a night.

Received 2008 September 10

1 The location

The following are recollections from a workshop on the meteoroid environment in near-Earth space held in Huntsville, Alabama, USA, from May 27 to 29, 2008. The organization of the meeting was led by Bill Cooke from the Meteoroid Environment Office (MEO) of the NASA Marshall Space Flight Center (MSFC) in Huntsville. The workshop venue, Jacobs Conference Center, offered really all you need for a successful meeting from coffee to presentation facilities.

Although not frequently visited by international flights, Huntsville is easily reached with numerous domestic connections. Flying into major cities such as Nashville, Memphis, or Birmingham and then driving to Huntsville does not take too long either. Huntsville is the home of the original Space Camp and the U.S. Space and Rocket Center. The 'Rocket City' is the place where rocket engineering and space flight were massively boosted, and as bonus to the workshop, it was interesting to sneak into the biography of German rocket engineer, Wernher von Braun. Von Braun was captured in the Second World War and brought to the United States to develop rockets. He became a leading figure in the rocket technology and space flight arenas in the U.S. without fully changing his authoritarian style of management he was used to when still in Germany.

2 How many particles are out there?

NASA programs are now requiring more rigorous evaluations of the meteoroid environment. The main aim of the workshop was to compare the various observing techniques with respect to their contribution to the 'meteoroid model' — a term which is used by spacecraft engineers to describe the distribution of meteoroids versus mass (or size) and velocity in the vicinity of Earth. Knowledge of the meteoroid flux as a function of these quantities at other places in the solar system is also desired, but much harder to obtain. The following selection of results and discussions are motivated by this aim, but conclusions for meteor science in general can, of course, be drawn as well.

One of the things that motivates the interest of spacecraft engineers in the meteoroid environment is the knowledge that spacecraft Mariner IV (1967), Olympus (1993), the HST (2002), Chandra (2003), and Stereo (2007) have been struck by meteoroids. These meteoroid hits were undesired, and in the case of Olympus, it ended the satellite's mission.

Impacts of interplanetary dust are desired when the particles hit a dust collector of an in-situ experiment. Bob Naumann, Yukihito Kitazawa, and Mark Matney reported on the current status of dust observations with their advantage of being the only direct measurement of the actual meteoroid environment and their disadvantage of providing only small numbers of events. The difficulty in determining the impact velocities was also discussed.

Numerical simulations of meteoroids were shown by Paul Wiegert and Jeremie Vaubaillon. Wiegert's talk addressed the origin and dynamics of the sporadic sources. An ensemble of Jupiter-family comets, Halley-type comets and main-belt asteroids was used to produce dust in various orbits — in total a sample of 250 million particles. Different families of parents are indeed found to be main contributors to different sporadic sources: Jupiter-family comets deliver the meteoroids for the antihelion and helion sources, Halley-type comets in retrograde orbits produce the northern and southern apex sources, while Halley-type comets in prograde orbits cause the northern and southern toroidal sources which are difficult to detect in the sample, however.

Dust from Comet 2P/Encke dominates the sporadic flux at sizes detectable by meteor patrol radars. We are not talking about the Taurid meteor shower which is a recent consequence of its dust production, but about the all-year-round sporadic source, which is also made of Encke dust while orbital nodes have spread over all solar longitudes during a hundred thousand years. At smaller sizes in the detection range of HPLA radar (High Power and Large Aperture), the sporadic flux is dominated by fast apex meteors, pointing to a possible resolution of the discrepancy between HPLA and meteor patrol radar velocity distributions. The asteroidal sources contribute to the sporadic sources only by a few percent. The sporadic sources are almost entirely cometary, not asteroidal, according to these results.

The thermal emission of dust in the zodiacal cloud reveals not a smooth distribution of dust, but the presence of a fine structure component known as the zodiacal cloud dust bands. These dust bands are known to be due to asteroidal sources and thus hold the key to determining the asteroidal component of the cloud.

[1] Friedenstr. 5, D-14109 Berlin, Germany. Email: rarlt@aip.de

[2] NASA Marshall Space Flight Center, Hunstville, Alabama 35812, USA. Email: danielle.e.moser@nasa.gov

IMO bibcode WGN-364-arlt-huntsville
NASA-ADS bibcode 2008JIMO...36...83A

Figure 1 – Meteoroid environment workshop in Huntsville, Alabama.

Figure 2 – Workshop organizer Bill Cooke (center) discussing with Margaret Campbell-Brown (left) and Peter Brown from the University of Western Ontario.

The dust bands can be well modeled and thus their specific asteroid sources are well known. Due to the effects of secular and mean-motion resonances, the band structure is constrained outside 2 AU, but the dust itself exists inwards to the Sun. Ashley Espy reported on preliminary modeling of the dust band structure and interpolation of the likely magnitude of dust inside of 2 AU, revealing that the asteroidal contribution to the cloud is probably less than 50%, with the remainder most likely stemming from cometary origin.

Since the critical point of all ground-based observations is the conversion of meteor numbers into particle numbers, the physics of the meteor phenomenon comes into play. If the conversion of the initial kinetic energy of the particle into other forms of energy could be known precisely, one could properly convert numbers into real fluxes and magnitudes into masses. We heard Douglas ReVelle speak about meteor physics in general and about the creation of infra-sound during the meteor flight, and how much energy it can carry away not being available to the luminous phenomenon. Pat Colestock showed impressive simulations of the plasma evolution during the ablation process of very small meteoroids. Remember that the conversion of meteor magnitudes into meteoroid masses still relies on the 35-year old relation derived by Verniani (1973).

Data calibration is another attempt to overcome the shortcomings of ground-based observations. Both video and radar systems are potentially the most powerful flux estimators, and a comprehensive project at the University of Western Ontario deals with simultaneous video and radar observations. Part of the project is the Automated Electro-Optical Meteor Observatory, presented by Robert Weryk. An all-sky system monitors the sky for meteors and a small telescope with high-speed positioning capabilities follows the meteor once it is detected. A video camera with up to 120 frames a second at VGA resolution records a sequence of meteor images. At a field of view of $1\overset{\circ}{.}5$, the resolution at meteor level is about 6 m per pixel. General issues of meteor photometry were discussed by Wesley Swift.

Jeremie Vaubaillon presented an overview of the various methods used for meteoroid stream modeling and stressed the need for observations in order to confirm the models. Among several examples of meteoroid stream evolution, Vaubaillon reported on the probability of enhanced Perseid rates in 2009 as a consequence of an oscillation-like motion of the orbital nodes of Perseid particles, which brings the stream closer to Earth every about 12 years — a result which is very similar to the expectations from the sun's reflex motion as shown by Jenniskens (1997). Another example was the π-Puppid stream fed by Comet 26P/Grigg Skjellerup which shows a totally distributed picture as of today. Vaubaillon does not expect enhanced rates from that shower in the near future. It looks like another example for a comet like Encke effectively feeding the sporadic background with particles ejected a long time ago.

A sensitive parameter in the models is the semi-major axis of the particles. If one wants to tackle the very interesting problem of pinning down the physics at the comet's nucleus by observations of the corresponding meteor shower on the Earth, the best measurement to achieve this is that of the semi-major axis. Precise determinations of a are therefore necessary – and these are often among the less well known. At least two decimals were quoted by Vaubaillon to be of any meaning for inverse conclusions from observations, rather than forward predictions.

3 Data resources

Meteoroid models all require flux and velocity observations that may be obtained by a variety of means. Various data sources providing information on the particle flux in the Earth's environment were discussed. Margaret Campbell-Brown gave details on the Canadian Meteor Orbit Radar (CMOR) in London, Ontario. About 5000 meteoroid orbits can be computed each day, with 95–96% of them being sporadic and having corresponding magnitudes of about +6 and +7. Peter Brown extended the view by computing the mass index from these sporadic meteors as $s = 2.34$ which is larger than the one obtained from the southern-hemisphere radar AMOR, $s \sim 2$. These numbers convert to $r \sim 3.8$ and $r \sim 2.7$, respectively, in terms of visual observers' population indices.

High-resolution radar observations using the AL-

TAIR facility were shown by Sigrid Close. Meteoroid velocities and densities were determined from the observations, the latter again employing some assumptions on the meteor physics, but resulting in an average of 0.6 g/cm^3 from 10 meteoroids. The trade-off for ALTAIR's accuracy and sensitivity is the smaller number of detections because granted observing time is limited at such a large and powerful telescope. Preliminary analysis on 30 hours of data taken in 2007/2008 is underway and more observations are planned.

A very accurate set of meteoroid orbits was derived by the meteor group using the EISCAT radar, a joint observatory of Sweden, Finland and Norway. According to the report by Gudmund Wannberg, these orbits appear to be exactly what stream modelers are after in order to discriminate the physical conditions at particle ejection from the comet and non-gravitational influences during their orbital evolution.

Pete Gural reported on the sporadic flux derived from the IMO Video Meteor Database. One of the authors (RA) reported on the status and capabilities of the Visual Meteor Database of the IMO as well as on the prospects of a virtual meteor observatory comprising data sets from a variety of observing methods. An international team led by the IMO will meet at the International Space Science Institute in Bern, Switzerland, in November 2008 in order to make progress with this project.

Figure 3 – Saturn V replica at the very impressive U.S. Space & Rocket Center in Huntsville.

4 Lunar impact observations

Rob Suggs gave a presentation about the NASA Lunar Impact Monitoring Program, which has been in operation since early 2006. The program makes Earth-based observations of the un-illuminated portion of the moon in order to determine the flux and sizes of large meteoroids striking the lunar surface. Observations are conducted when the solar illumination is between 10 and 50%, yielding several observing nights per month. The program utilizes StellaCam Ex and Watec 902H2 Ult cameras on three telescopes: 35-cm and 50-cm telescopes in Huntsville at MSFC, and a 35-cm in Chickamauga, Georgia. To date, the program has detected over 125 impact flashes on the moon, the majority of which have been observed by at least two telescopes (and many by three). The data imply an average of more than three kg-class sporadic impacts per hour somewhere on the moon during non-shower periods.

The NASA camera covers a $20'$-field on the dark side of the Moon. The flashes are faint; an example of one of the brightest events is a magnitude +6.86 flash that lasted about 500 ms. An estimate of the energy release leads to a crater size of 10–15 m. This size crater is too small to be seen in any amateur telescope (0.1" are about 180 m on the Moon). The resolution of the system is too poor to determine a location accurately enough for a crater search with a large telescope. The results are therefore statistical in nature; impact rates and intensities can reveal direct information on the meteoroid environment near the Earth. In order to be significant, these results must be based on a considerable number of observations. A world-wide network of lunar-impact monitoring is the preferred solution, of course. We would like to encourage observers to consider this field of meteor observations.

It must be noted that this type of observation requires a technical setup, however, because visual searches for impact flashes have not been very successful in the past. The website of NASA's Lunar Impact Monitoring Program, `http://www.nasa.gov/centers/marshall/news/lunar/` provides a document on the type of system required to make lunar impact observations. From this website you can also download LunarScan, an impact flash search program developed by Pete Gural with funding provided by the NASA MEO. Observers may report their impact candidates through this website and also reference the list of candidates observed at MSFC.

George Varros reported on his lunar-impact observations in Maryland which often runs parallel to the program at MSFC. He operates a StellaCam II camera on a 20-cm telescope and has confirmed three events seen by the NASA monitoring program, the duration of each lasting between one and three video frames.

5 The 2011 Draconids

Predictions, geometrical conditions, and weather statistics for the 2011 Draconids were evaluated and presented by one of the authors (DM). Possible meteor activity peaks are likely to fall between 19^h11^m and 20^h42^m UT on 2011 October 08, according to particle simulations by Maslov, Moser, Vaubaillon, and Watanabe & Sato. Cloud statistics are best for northern Africa, whereas geometrical conditions are best in central Europe. A 91% illuminated Moon disturbs all imaging observations. A high-altitude location seems suitable to reduce the influence from stray-light due to haze. Assuming that the timing of the predictions is of fair accuracy, one may choose a location in western Europe to see the radiant highest in the sky. A reasonable combination of weather, geometry, and high-altitude points to the observatories in southern Spain.

Acknowledgements

RA would like to thank Bill Cooke for the invitation to this very interesting and productive meeting. We also thank Ashley Espy and Paul Wiegert for their helpful information.

References

Jenniskens P. (1997). "Meteor stream activity. IV. Meteor outbursts and the reflex motion of the Sun". *Astron. Astrophys.*, **317**, 953.

Verniani F. (1973). "An analysis of the physical parameters of 5759 faint radio meteors". *J. Geophys. Res.*, **78**, 8429–8462.

Preliminary results

Results of the IMO Video Meteor Network — May 2008

Sirko Molau [1] *and Javor Kac* [2]

Up to now, May was the month were we had recorded least meteors. Between 1993 and 2007, only 10 002 shooting stars were captured by our video network. That picture has changed, however, thanks to the exceptional weather this year. In the first half of May, there were essentially clear skies at each observing site. We have nine cameras that could observe in 13 or more of the first 15 May nights (Table 1 and Figure 2). The weather changed rapidly in the second half of the month, when we had the typical mix of clouds and rain, but overall we recorded more than 3500 meteors in more than 1500 hours of effective observing time. That's about twice as many observing hours and two third more meteors as in 2007, the best year so far. Hence, May has now overtaken June, from which we have 11 680 records in the video meteor database. It remains to see, how the distribution looks like after the next month.

With the eta-Aquariids there is a major shower early May, which, however, is difficult to observe from northern latitudes where most cameras are located. So it is no surprise that the following minor shower of the eta-Lyrids seemed to have about the same activity. This impression is supported by an analysis, where the number of shower meteors is summed up for each night and normalized by the number of sporadics in the same night. The eta-Aquariids show an activity profile with a broad maximum between May 4 and May 9 (Figure 1). At

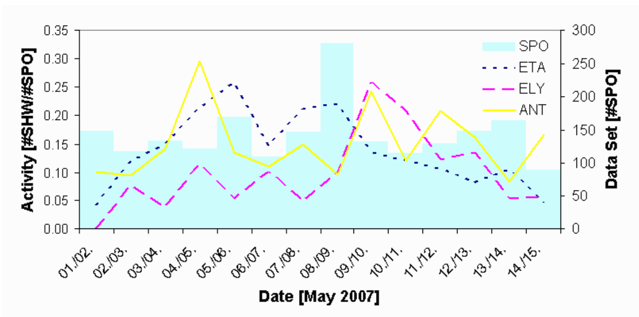

Figure 1 – Activity profiles of the eta-Aquariids, eta-Lyrids, and the Antihelion source in the first half of May.

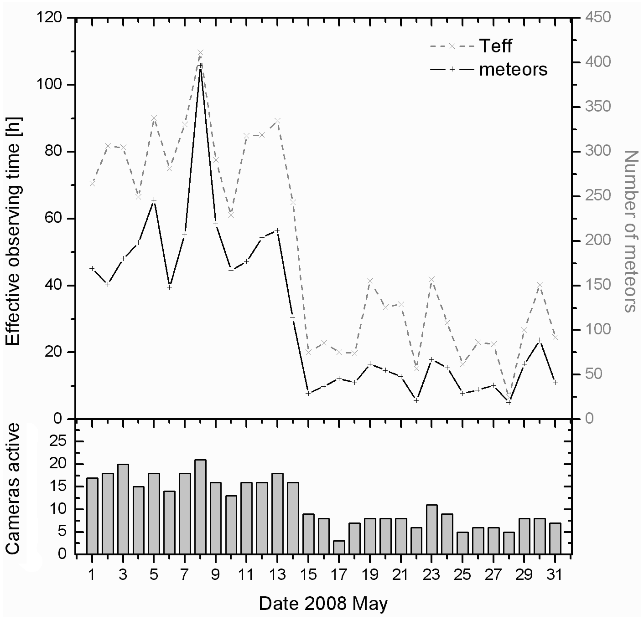

Figure 2 – Monthly summary for the effective observing time (dashed gray line), number of meteors (solid black line) and number of cameras active (bars) in May 2008.

maximum their count was about a quarter of the sporadic count. The profile of the eta-Lyrids has a more compact maximum between May 9 and May 11, where they also reach about a quarter of the sporadic count.

Which influence does the observing geometry have? The observability function (that is the integral over the sine of the radiant altitude in the course of the night) of the showers for a mean latitude of 48° N yields an observation probability of about 5% for the eta-Aquariids, 31% for the Antihelion source, and 74% for the eta-Lyrids. That reflects, that the eta-Aquariids radiant rises only at dawn, whereas the radiant of the eta-Lyrids in high up in the sky all night long. If we now set the maximum ZHR of the eta-Aquariids to 50, we get a corrected average ZHR estimates of the Antihelion source below 20, and a peak eta-Lyrids ZHR estimate of about 3. That's much closer to the expected values.

[1] Abenstalstr. 13b, 84072 Seysdorf, Germany.
Email: `sirko@molau.de`
[2] Na Ajdov hrib 24, 2310 Slovenska Bistrica, Slovenia.
Email: `javor.kac@orion-drustvo.si`

IMO bibcode WGN-364-molau-vidmay
NASA-ADS bibcode 2008JIMO...36...87M

Table 1 – Observers contributing to May 2008 data of the IMO Video Meteor Network.

Code	Name	Place	Camera	FOV	LM	Nights	Time (h)	Meteors
BENOR	Benitez-S.	Las Palmas	TIMES4 (1.4/50)	⊘ 20°	3 mag	3	1.1	5
			TIMES5 (0.95/50)	⊘ 10°	3 mag	2	0.3	2
BRIBE	Brinkmann	Herne	HERMINE (0.8/6)	⊘ 55°	3 mag	22	106.7	162
CASFL	Castellani	Monte Baldo	BMH1 (0.8/6)	⊘ 55°	3 mag	17	52.5	102
			BMH2 (0.8/6)	⊘ 55°	3 mag	9	24.2	35
CRIST	Crivello	Valbrevenna	STG38 (0.8/3.8)	⊘ 80°	3 mag	2	12.9	20
ELTMA	Eltri	Venezia	MET38 (0.8/3.8)	⊘ 80°	3 mag	3	20.1	61
GONRU	Goncalves	Tomar	TEMPLAR1 (0.8/6)	⊘ 55°	3 mag	12	62.4	72
HERCA	Hergenrother	Tucson	SALSA (1.2/4)	⊘ 80°	3 mag	22	151.2	191
HINWO	Hinz	Brannenburg	AKM2 (0.85/25)	⊘ 32°	6 mag	18	84.8	206
KACJA	Kac	Kostanjevec	METKA (0.8/8)	⊘ 42°	4 mag	15	75.5	127
		Kamnik	REZIKA (0.8/6)	⊘ 55°	3 mag	6	36.5	98
		Ljubljana	ORION1 (0.8/8)	⊘ 42°	4 mag	20	82.4	124
KOSDE	Koschny	Noord-wijkerhout	ICC4 (0.85/25)	⊘ 25°	5 mag	10	40.9	83
LUNRO	Lunsford	Chula Vista	BOCAM (1.4/50)	⊘ 60°	6 mag	14	64.7	270
MOLSI	Molau	Seysdorf	AVIS2 (1.4/50)	⊘ 60°	6 mag	15	80.8	739
			MINCAM1 (0.8/6)	⊘ 60°	3 mag	19	103.7	162
		Ketzuer	REMO1 (0.8/3.8)	⊘ 80°	3 mag	21	112.0	176
			REMO2 (0.8/3.8)	⊘ 80°	3 mag	6	24.6	69
PRZDA	Przewozny	Berlin	ARMEFA (0.8/6)	⊘ 55°	3 mag	14	79.1	156
SLAST	Slavec	Ljubljana	KAYAK1 (1.8/28)	⊘ 50°	4 mag	14	52.5	87
STOEN	Stomeo	Scorze	MIN38 (0.8/3.8)	⊘ 80°	3 mag	11	54.2	152
STRJO	Strunk	Herford	MINCAM2 (0.8/6)	⊘ 55°	3 mag	24	60.7	89
			MINCAM3 (0.8/8)	⊘ 42°	4 mag	17	39.0	63
			MINCAM5 (0.8/6)	⊘ 55°	3 mag	20	82.7	165
WEBMI	Weber	Chouzava	TOMIL (1.4/50)	⊘ 50°	6 mag	4	5.6	86
YRJIL	Yrjola	Kuusankoski	FINEXCAM (0.8/6)	⊘ 55°	3 mag	18	52.4	62
					Overall	31	1563.5	3564

Results of the IMO Video Meteor Network — June 2008

Sirko Molau [1] *and Javor Kac* [2]

Due to the short northern nights, the effective observing time dropped to little above thousand hours in June, which is the lowest value so far in 2008 (Table and Figure 1). However, that result should not discourage us. On the one hand, the data of the two remotely operated cameras Remo1 and Remo2 are not yet included, and on the other hand we never managed to get beyond 680 hours in all the previous years. Especially Rui Concalves and Carl Hergenrother, who have been contributing to the IMO network since early this year, enjoy many clear nights thanks to their excellent observing sites, but also the weather was favourable in the second half of June.

Was that sufficient to bring May back to the last place in the overall statistics? Yes! The number of meteors was significantly smaller than in the last month, but still it was sufficient for a head start of 500 meteors compared to May. Also the June and July meteors of 2008 will be included in the next full analysis of the video meteor database, which will be presented at the IMC.

By the way, it is clearly visible how the activity has risen again in the last few days of June. Whereas the average hourly count was two meteors, it jumped to three to four meteors per hour in the last three nights on June. The meteor season has started again!

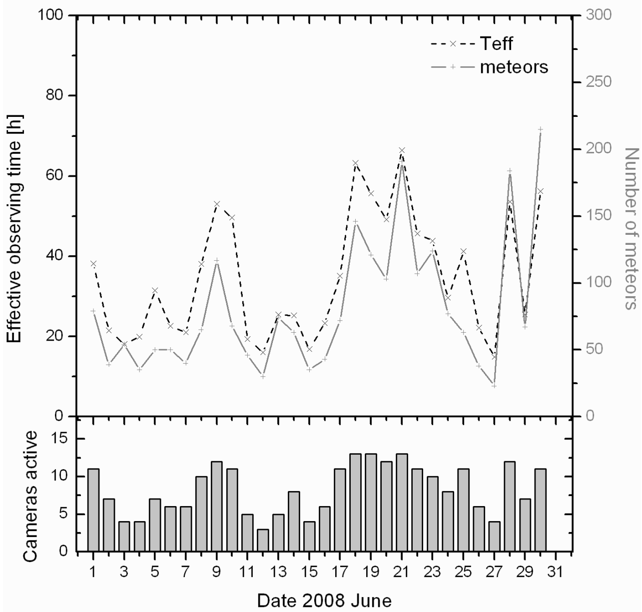

Figure 1 – Monthly summary for the effective observing time (dashed gray line), number of meteors (solid black line) and number of cameras active (bars) in June 2008.

Table 1 – Observers contributing to June 2008 data of the IMO Video Meteor Network.

Code	Name	Place	Camera	FOV	LM	Nights	Time (h)	Meteors
BRIBE	Brinkmann	Herne	HERMINE (0.8/6)	⊘ 55°	3 mag	24	71.7	201
CASFL	Castellani	Monte Baldo	BMH1 (0.8/6)	⊘ 55°	3 mag	13	49.7	75
			BMH2 (0.8/6)	⊘ 55°	3 mag	12	39.7	52
CRIST	Crivello	Valbrevenna	STG38 (0.8/3.8)	⊘ 80°	3 mag	4	19.4	61
GONRU	Goncalves	Tomar	TEMPLAR1 (0.8/6)	⊘ 55°	3 mag	24	140.3	240
HERCA	Hergenrother	Tucson	SALSA (1.2/4)	⊘ 80°	3 mag	23	168.0	255
HINWO	Hinz	Brannenburg	AKM2 (0.85/25)	⊘ 32°	6 mag	14	54.1	116
KACJA	Kac	Kostanjevec	METKA (0.8/8)	⊘ 42°	4 mag	8	40.7	56
		Kamnik	REZIKA (0.8/6)	⊘ 55°	3 mag	8	39.5	107
		Ljubljana	ORION1 (0.8/8)	⊘ 42°	4 mag	16	68.3	96
LUNRO	Lunsford	Chula Vista	BOCAM (1.4/50)	⊘ 60°	6 mag	11	70.1	255
MOLSI	Molau	Seysdorf	AVIS2 (1.4/50)	⊘ 60°	6 mag	17	54.8	402
			MINCAM1 (0.8/6)	⊘ 60°	3 mag	20	70.4	126
PRZDA	Przewozny	Berlin	ARMEFA (0.8/6)	⊘ 55°	3 mag	6	26.8	68
SLAST	Slavec	Ljubljana	KAYAK1 (1.8/28)	⊘ 50°	4 mag	5	16.3	36
STOEN	Stomeo	Scorze	MIN38 (0.8/3.8)	⊘ 80°	3 mag	11	44.6	101
STRJO	Strunk	Herford	MINCAM2 (0.8/6)	⊘ 55°	3 mag	19	29.6	59
			MINCAM3 (0.8/8)	⊘ 42°	4 mag	6	13.8	23
			MINCAM5 (0.8/6)	⊘ 55°	3 mag	8	20.0	44
WEBMI	Weber	Chouzava	TOMIL (1.4/50)	⊘ 50°	6 mag	2	3.8	46
					Overall	30	1041.6	2419

[1] Abenstalstr. 13b, 84072 Seysdorf, Germany.
Email: sirko@molau.de
[2] Na Ajdov hrib 24, 2310 Slovenska Bistrica, Slovenia.
Email: javor.kac@orion-drustvo.si

IMO bibcode WGN-364-molau-vidjun
NASA-ADS bibcode 2008JIMO...36...89M

Results of the IMO Video Meteor Network — July 2008

Sirko Molau [1] *and Javor Kac* [2]

From the viewpoint of the weather, July was comparable with the month before: It was not perfect, but there is no reason to complain if nine cameras managed to collect twenty or more observing nights. Especially in the last few days of July the skies were clear at almost every site, so that at times more than twenty cameras were operated in parallel (Figure 1 and Table 1). Needless to say that we could collect more observing times and meteors than in any other July before.

The increasing meteor activity – mainly thanks to the alpha-Capricornids and southern delta-Aquariids – was highly welcome. At mid-July first Perseids became visible. They are a minor shower at the beginning, but towards the end of July they became dominating. Only the southern delta-Aquariids could catch up with the Perseid counts in the days of their maximum around July 28. A nice example for an SDA radiant plot was provided by TOMIL, the camera of Tomas and Milos Weber (Figure 2, left frame). It was able to record 63 meteors (including 11 SDA) within just two hours on July 27/28 thanks to the powerful image intensifier. Rosta Stork of Ondrejov enjoyed even better observing conditions in the next night, when he recorded 273 meteors (among them 33 SDA) in less than six hours (Figure 2, right frame).

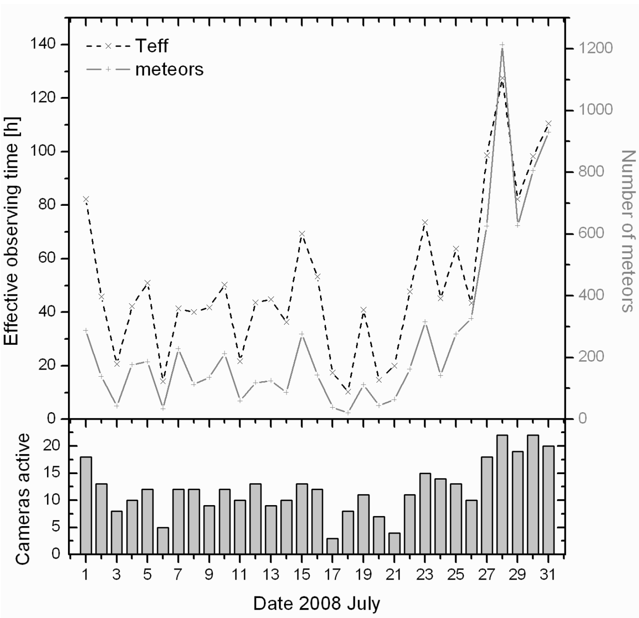

Figure 1 – Monthly summary for the effective observing time (solid black line), number of meteors (dashed gray line) and number of cameras active (bars) in July 2008.

[1] Abenstalstr. 13b, 84072 Seysdorf, Germany. Email: sirko@molau.de

[2] Na Ajdov hrib 24, 2310 Slovenska Bistrica, Slovenia. Email: javor.kac@orion-drustvo.si

IMO bibcode WGN-364-molau-vidjul
NASA-ADS bibcode 2008JIMO...36...90M

The 'most beautiful' meteor of the month, however, was captured by Stefano Crivello, who recorded a double Capricornid on July 27 at 01:55 UT (Figure 3).

Beside archiving the July data also the next full analysis of the video meteor database was prepared in the last few days. In particular the scatter respectively observing errors of video meteors with respect to position and angular velocity was of interest. As explained before, the meteor shower analysis relies on the accumulation of probabilities, that meteors origin from a particular radiant with given position and velocity. That probability is derived from two quantities – the distance at which the backward prolongation of the meteor misses the (point-like) radiant, and the difference between the observed and the expected angular velocity. The latter one is calculated from the distance of the meteor from the radiant, and the meteor shower velocity.

Those who have used the Radiant software of Rainer Arlt know the phenomenon: With the parameter 'Standard Deviation' you can adjust whether the probability distribution of a meteor in probability mode becomes a small droplet (small scatter, the radiation area can be well defined) or a large area (large scatter, the radiant can be determined only approximately). You need to adjust the settings by trial and error: when the standard deviation is set too small, random sub-radiants will show up, whereas a meteor shower radiant becomes blurred, when the standard deviation is set too large.

In the 2006 analysis I had chosen both for the scatter in angular velocity and radiant distance a normal (Gaussian) distribution. The standard deviation was set empirically to a 'sensible' value. This time, the standard deviation was to be computed from data. For this reason, short intervals in solar longitude at the maximum times of the Perseids, Orionids, and Geminids were chosen, in which the radiant was compact and showed only little drift. Then all shower members in these solar longitude intervals were determined (more than 33 000 meteors overall) and the distributions were computed, how the angular meteor velocity differed from the expected value and how far the backward prolongation missed the radiant. In addition, the dependency of these distributions from the angular velocity of the meteor and its distance from the radiant was analysed.

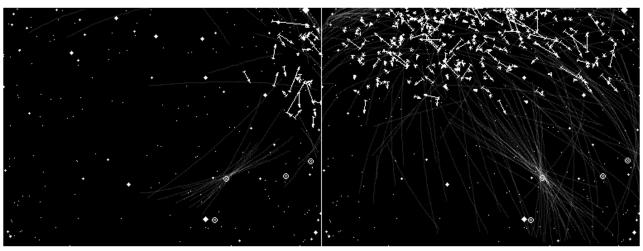

Figure 2 – The radiant plots of TOMIL (left) from July 27/28 and OND1 (right) from July 28/29 show nicely the radiant of the southern delta-Aquariids.

Here is a summary of the results:

- On average, the scatter is lower than expected. The observed angular velocity of half of all meteors deviates less than half a degree per second from the expected value (whereby the underlying PosDat database contains only integer values for the velocity, anyway), and the backward prolongation missed the radiant by less than three quarter of a degree. At one sigma (68.3%) the deviation is 0.8°/s and 1.3°.
- Ihe distributions are not Gaussian as expected, but can be well described by a Laplace distribution (i.e. a function of the type e^{-x} instead of e^{-x^2}). The main difference is, that for large values the Laplace function converges much slower to zero than the Gauss function.
- There is a clear dependency between the scatter in angular velocity and the meteor velocity (the faster the meteors, the large the scatter – the scatter for meteors that move faster than 30 deg/s is about twice as large as for meteors slower than 10 deg/s). On the other hand, the scatter of the radiant miss distance of the backward prolongations is essentially independent from the distance of the meteor from the radiant.
  The IMO handbook for meteor observers, by the way, suggests that in the analysis of visual observation larger errors should be accepted both for the angular velocity and the radiant miss distance for meteors that are fast or far away from the radiant.

Figures 4 and 5 show the cumulative distributions for those 33 000 Perseids, Orionids and Geminids.

Figure 3 – Double Capricornid, recorded by Stefano Crivello with STG38 on July 27, 01:55 UT.

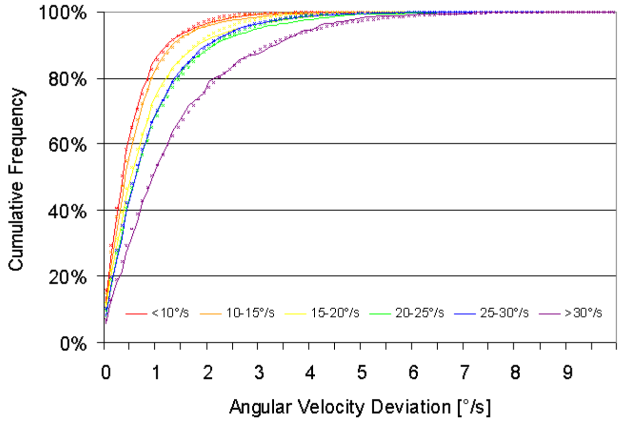

Figure 4 – Cumulative distribution of velocity errors for different angular velocities of meteors. Small crosses mark the corresponding Laplace fits.

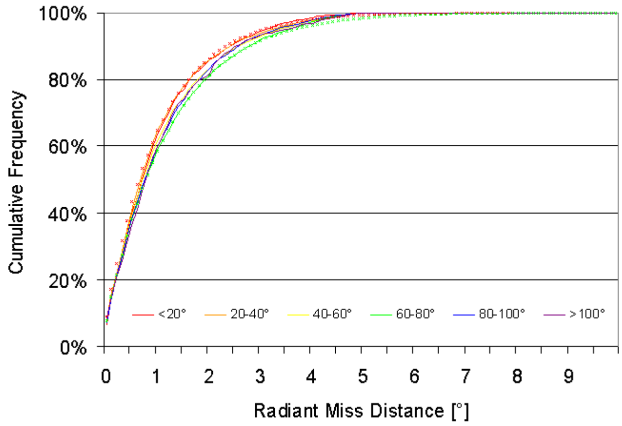

Figure 5 – Cumulative distribution of radiant miss distances for different distances of the meteor from the radiant. Small crosses mark an lower and upper Laplace fit.

Ironically, when I carried out the meteor database analysis for the first time before the AKM spring meeting 2006, I accidentally used a Laplace distribution. Later I noticed this 'error' and used a normal distribution for the analysis later presented at the 2006 IMC – as one usually does if the true probability distribution is unknown. Now it turns out that the Laplace distribution would have been better. The influence of the distribution is not as dramatic, however, that we may expect completely different results now. At least the next analysis will not be done with empirically set parameters, but with a probability distribution derived from data, so from the point of view of probability theory everything is fine.

Strictly speaking, the distributions models only the scatter for compact radiants. If the radiation area is of bigger size, the distribution should be wider as well – but that's a different topic.

Table 1 – Observers contributing to July 2008 data of the IMO Video Meteor Network.

Code	Name	Place	Camera	FOV	LM	Nights	Time (h)	Meteors
BENOR	Benitez-S.	Las Palmas	TIMES4 (1.4/50)	⊘ 20°	3 mag	5	33.5	93
			TIMES5 (0.95/50)	⊘ 10°	3 mag	5	18.4	34
BRIBE	Brinkmann	Herne	HERMINE (0.8/6)	⊘ 55°	3 mag	23	75.6	252
CASFL	Castellani	Monte Baldo	BMH1 (0.8/6)	⊘ 55°	3 mag	21	88.9	278
			BMH2 (0.8/6)	⊘ 55°	3 mag	27	95.4	261
CRIST	Crivello	Valbrevenna	STG38 (0.8/3.8)	⊘ 80°	3 mag	4	14.9	64
ELTMA	Eltri	Venezia	MET38 (0.8/3.8)	⊘ 80°	3 mag	3	19.7	123
GONRU	Goncalves	Tomar	TEMPLAR1 (0.8/3.8)	⊘ 80°	3 mag	27	161.1	451
HERCA	Hergenrother	Tucson	SALSA (1.2/4)	⊘ 80°	3 mag	15	73.0	229
HINWO	Hinz	Brannenburg	AKM2 (0.85/25)	⊘ 32°	6 mag	11	41.1	206
KACJA	Kac	Kostanjevec	METKA (0.8/8)	⊘ 42°	4 mag	11	64.2	187
		Kamnik	REZIKA (0.8/6)	⊘ 55°	3 mag	8	38.5	165
		Ljubljana	ORION1 (0.8/8)	⊘ 42°	4 mag	23	103.9	297
LUNRO	Lunsford	Chula Vista	BOCAM (1.4/50)	⊘ 60°	6 mag	22	89.5	1031
MOLSI	Molau	Seysdorf	AVIS2 (1.4/50)	⊘ 60°	6 mag	13	55.9	955
			MINCAM1 (0.8/6)	⊘ 55°	3 mag	19	84.9	273
		Ketzuer	REMO1 (0.8/3.8)	⊘ 80°	3 mag	24	91.5	412
			REMO2 (0.8/3.8)	⊘ 80°	3 mag	24	88.5	439
PRZDA	Przewozny	Berlin	ARMEFA (0.8/6)	⊘ 55°	3 mag	14	69.5	428
SLAST	Slavec	Ljubljana	KAYAK1 (1.8/28)	⊘ 50°	4 mag	20	78.4	154
STOEN	Stomeo	Scorze	MIN38 (0.8/3.8)	⊘ 80°	3 mag	13	73.9	291
STORO	Stork	Kunzak	KUN1 (1.4/50)	⊘ 55°	6 mag	2	11.5	253
		Ondrejov	OND1 (1.4/50)	⊘ 55°	6 mag	4	21.3	693
STRJO	Strunk	Herford	MINCAM2 (0.8/6)	⊘ 55°	3 mag	14	32.8	86
			MINCAM3 (0.8/8)	⊘ 42°	4 mag	5	19.2	66
			MINCAM5 (0.8/6)	⊘ 55°	3 mag	11	34.9	113
WEBMI	Weber	Chouzava	TOMIL (1.4/50)	⊘ 50°	6 mag	6	10.9	237
YRJIL	Yrjola	Kuusankoski	FINEXCAM (0.8/6)	⊘ 55°	3 mag	1	1.8	7
					Overall	31	1592.7	8078

The International Meteor Organization

web site http://www.imo.net

Council

Commission Directors

WGN

IMO Sales

Available from the Treasurer or the Electronic Shop on the IMO Website	€	$
IMO membership, including subscription to WGN Vol. 36 (2008)		
Surface mail	26	36
Air Mail (outside Europe only)	49	69
Corporate subscription to WGN Vol. 36 (2008)		
Surface mail	50	70
Air Mail (outside Europe only)	73	103
Back issues of WGN on paper		
Vols. 26 (1998) – 34 (2006) except 30 (2002), per complete volume	15	21
Proceedings of the International Meteor Conference on paper		
1990, 1991, 1993, 1995, 1996, 1999, 2000, 2002, 2003, 2004, per year	10	14
2005	15	21
Proceedings of the Radio Meteor School on paper		
2005 *(Reprinted — available again)*	15	21
Electronic media		
DVD: WGN Vols. 6–30 & IMC 1991, 1993–96, 2001–04	45	63

Readers' meteors

A long meteor from Miloš Weber. Locality: Chouzava, 14.°541100 E, 49.°835300, altitude 420 m. Taken on 2007 June 13 at $23^{\rm h}04^{\rm m}40^{\rm s}$ UT. Camera with intensifier, lens $f/1.4$, $f = 50$ mm. Meteor data: $m = -0.3$, velocity 17.5°/s, length 42.°6. Shower: SPO.

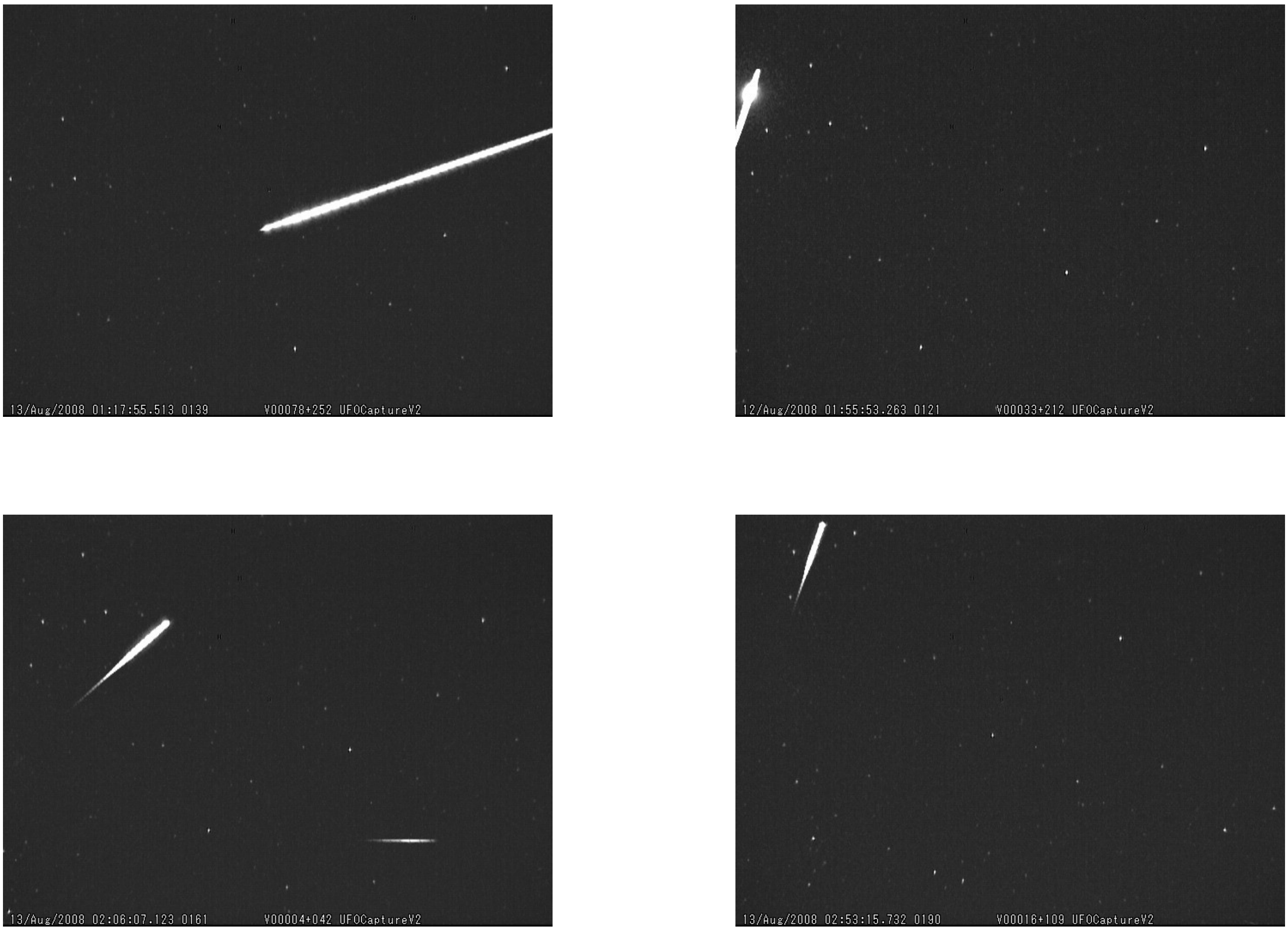

Video frames of a Capricornid (top left) and three Perseids.
Recorded on the nights of 2008 August 11/12 and 12/13. Photos by Roberto Haver.